AD-A053 350 AIR FORCE INST OF TECH WRIGHT-PATTERSON AFB OHIO SCH--ETC F/G 17/8
A SPECKLE NOISE MODEL FOR OPTICAL HETERODYNE LINE-SCAN IMAGERY.(U)
DEC 77 B W LYONS

UNCLASSIFIED AFIT/GEO/EE/77-4 NL

1 OF 1
AD A053350





END
DATE FILMED
6-78
DDC

AD A053350

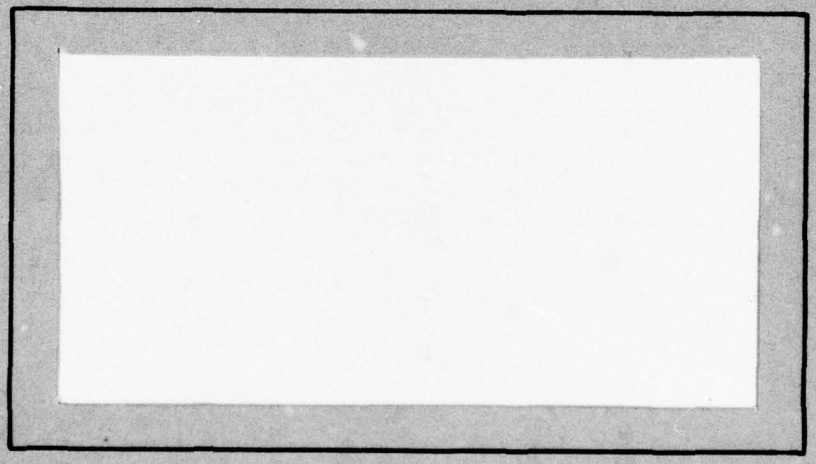
(1)

AIR FORCE INSTITUTE OF TECHNOLOGY



AIR UNIVERSITY
UNITED STATES AIR FORCE

AD No. ____
DDC FILE COPY



SCHOOL OF ENGINEERING

DDC
RECEIVED
MAY 2 1978
A

WRIGHT-PATTERSON AIR FORCE BASE, OHIO

DISTRIBUTION STATEMENT A
Approved for public release;
Distribution Unlimited

AFIT/GEO/EE/77-4

(1)

AD A053350

AD No.
DDC FILE COPY

A SPECKLE NOISE MODEL FOR OPTICAL HETERODYNE LINE-SCAN IMAGERY

THESIS

AFIT/GEO/EE/77-4 Barry W. Lyons
Capt USAF

Approved for public release; distribution unlimited.

DDC
RECEIVED
MAY 2 1978
A

(14) AFIT/GEO/EE/77-4

(6) A SPECKLE NOISE MODEL FOR OPTICAL HETERODYNE LINE-SCAN IMAGERY.

(9) Master's THESIS

Presented to the Faculty of the School of Engineering

of the Air Force Institute of Technology

Air University

in Partial Fulfillment of the

Requirements for the Degree of

Master of Science

(12) 74 p.

by

(10) Barry W. Lyons, B.S.

Capt USAF

Graduate Electro-Optics

(11) December 1977

ACCESSION for
NTIS White Section
DDC Buff Section
UNANNOUNCED
JUSTIFICATION
BY
DISTRIBUTION/AVAILABILITY CODES
Dist. AVAIL. and/or SPECIAL
A

Approved for public release; distribution unlimited.

012 225

Preface

This thesis was sponsored by the Air Force Avionics Laboratory at Wright-Patterson Air Force Base, Ohio. In this thesis, a model of an optical heterodyne line-scan imaging system is developed, which includes the effects of image distortion due to speckle. The model that is developed describes both the speckle cell size in the image and the contrast in the image caused by speckle.

I would like to thank Dr. B. L. Sowers, the individual sponsor at the Avionics Laboratory, for his suggestions and support. I would also like to thank Mr. W. C. Schoonover of the Avionics Laboratory for the office space he provided. I must thank my fellow classmates, Capts J. B. Armor, H. E. Hagemeier, R. S. Shinkle, and W. D. Strautman, for their many helpful discussions. I also offer a very sincere, "Thank You", to my AFIT thesis advisor, Capt S. R. Robinson for his encouragement and very competent technical guidance. The patience and understanding of my wife, Sharon, and my children, Greg and Sarah, during this nine month period is deeply appreciated. Finally, I would like to thank Debi Walters for her work in typing this thesis.

Contents

	Page
Preface	ii
List of Figures and Tables	iv
Abstract	v
I. Introduction	1
II. Background	4
Speckle	4
Huygens-Fresnel Integral	5
Fresnel Approximation	9
Fraunhofer Approximation	9
One-Dimensional Huygens-Fresnel Integral	10
Propagation and Relfection of a Laser Beam	11
Statistics in Modeling	12
Measurement of Optical Signals	15
Direct Detection	17
Heterodyne Detection	18
III. The System Model	21
The Rough Surface Phase Model	21
The Heterodyne Detector Current Model	26
The Real Current	26
The Complex Current	31
The Signal Detection Models	39
The Quadrature Model	40
Background Theory for Detection of A and A^2	42
The Model for Detection of A^2	45
The Model for Detection of A	51
IV. Summary	56
Conclusions	56
Recommendations	60
Bibliography	62
Vita	64

List of Figures and Tables

Figure		Page
1	The Optical Heterodyne Line-scan Imaging System	2
2	The Magnitude of $F_t u(\bar{r},t)$	6
3	Diffraction Geometry (Ref 7:57)	8
4	Illustrations of Typical Statistical Relationships	16
5	Model for Determining the Path Differences Induced by the Rough Surface	23
6	System Geometry	28
7	Plot of $P_\ell(\Delta\alpha)$	34
8	Comparison of $\alpha^2-\alpha'^2$ to $\alpha-\alpha'$	35
9	Graphical Determination of the Complex Current Correlation Distance	37
10	The Quadrature Model	40
11	Determination of A and A^2 from the Quadrature Outputs	43
12	The Model for Detection of the Current Amplitude Squared	46
13	The Approximated Model for Detection of the Current Amplitude	55

Table		
I	Values of Surface Roughness (Ref 15:859)	24

Abstract

An imaging system that consists of a laser scanning a surface and a heterodyne receiver that measures the backscattered field is considered. When the scanned surface is rough compared to the wavelength of the incident laser beam the coherent properties of the laser beam are destroyed in the backscattered field. This incoherence induces a noise in the resulting image that is commonly referred to as "speckle".

The rough surface is modeled crudely by multiplying the incident scalar field by a reflectance term and a random phase term. The reflectance is the "signal" that is desired to be measured. The two dimensional fields are propagated from one plane to another through the Huygens-Fresnel integral. The random phase is considered to be a zero mean stationary Gaussian random process whose variance and correlation distance are a function of the rough surface. It is shown that the correlation function of the field is very narrow when the field is reflected from surfaces that are rough compared to the optical wavelength. A complex current representation is used to show that the mean of the output from the optical detector is zero. However, the statistics of the amplitude and amplitude squared of the current do result in a mean "signal" and they are developed in a manner similar to the well known narrowband noise model. Second moment models for detection of the amplitude

of the current and for detection of the amplitude squared of the current are presented. The mean "signal" and covariance "noise" functions are related to the field correlation function, the reflectance of the surface, and the system parameters. The system parameters include the scanning velocity, the Gaussian laser beam spot size, the receiver aperture size, the optical wavelength, and the observation distance. The noise models describe both the average speckle cell size in the image and the contrast in the image that is due to the speckle noise. It is shown that the form of the model is the same for both the far field and near field cases. The models developed in this thesis provide a basis for determining the "optimum" signal processing method for producing the "best" image quality.

A SPECKLE NOISE MODEL FOR OPTICAL HETERODYNE LINE-SCAN IMAGERY

I. Introduction

The objective of this thesis is to analyze an optical heterodyne line-scan imaging system for the case of rough surface reflection. Fig. 1 is an illustration of the system with an accompanying simple block diagram. The models developed in this thesis will include all but the final two blocks shown in Fig. 1. In the system a laser illuminator scans the object surface in a pattern that will result in complete "once only" coverage of a certain area. The scanning system also reflects the field backscattered from each illuminated spot onto an optical heterodyne detector as the beam is scanned over the surface. The backscattered field is a function of the reflectivity of the object's surface therefore, an image of the surface can be obtained from the detected field. If the object's surface is optically smooth then specular reflection will occur and the field will not be reflected directly back to the detector except when the beam is normally incident on the object surface. However most surfaces are rough with respect to optical wavelengths so that a portion of the field is constantly backscattered to the detector. While this rough surface provides the energy needed for detection it also distorts the reflected wave and the resulting image because the exact form of the surface roughness is "a priori"

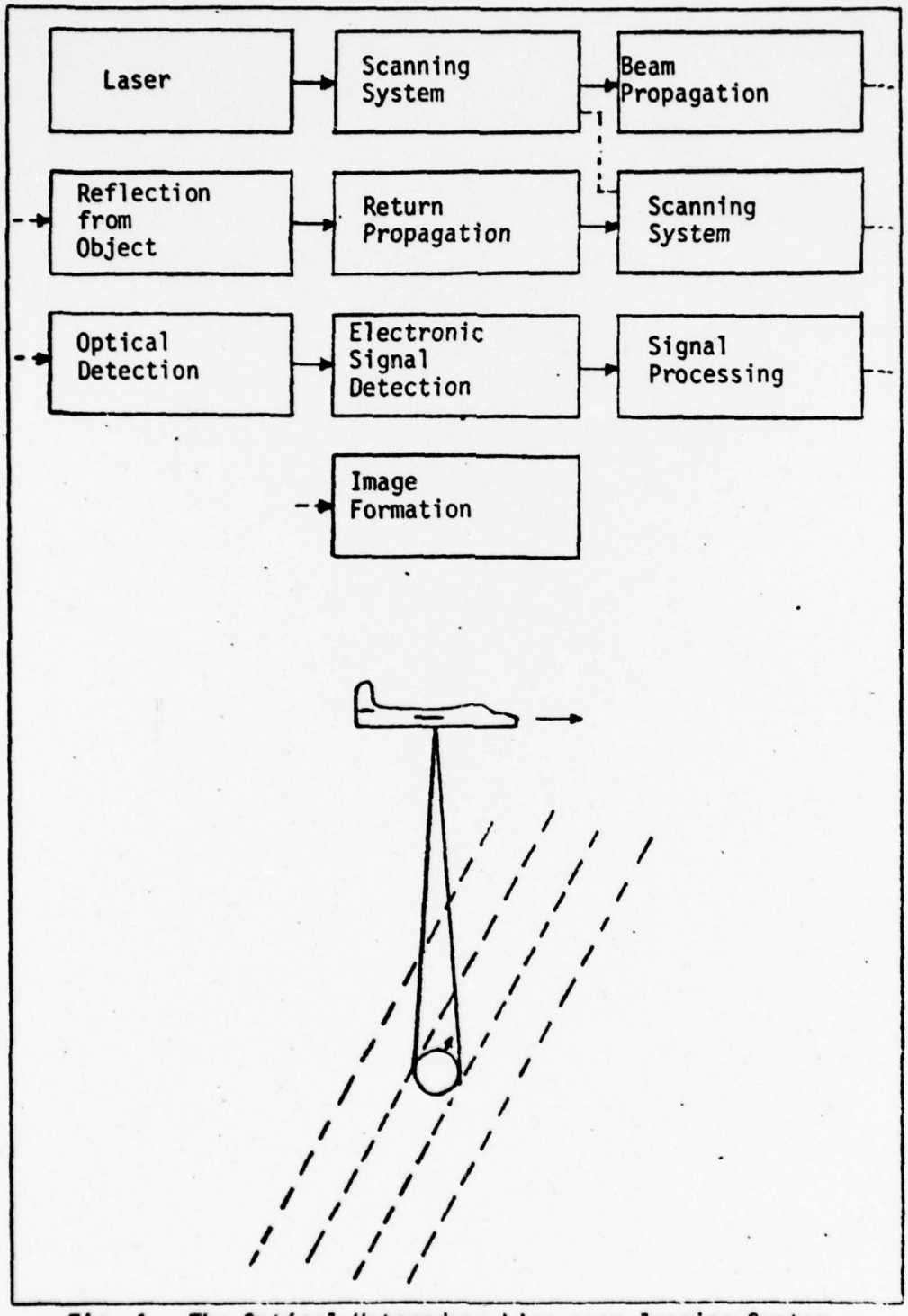


Fig. 1. The Optical Heterodyne Line-scan Imaging System

unknown and constantly changing as the beam is moved to different areas. This image distortion is commonly called "speckle".

In this thesis all optical fields will be considered monochromatic or quasimonochromatic and will be mathematically propagated from one point to another by using the Huygens-Fresnel integral. The rough surface will be modeled using statistics and the optical detector output current will be based on known detector models. The resulting statistics of the detector output current will be used in modeling two methods of signal detection. The statistics of the final detected signal will be a function of the system parameters such as the laser beam spot size, the scanning velocity, the detector aperture size, and the optical local oscillator field. The effect of the parameters on the reflectivity "signal" and the speckle "noise" will be discussed within the context of each model.

First the background necessary for development of the system model will be presented. Then the system model will be developed and finally the two types of signal detection models will be presented and discussed.

II BACKGROUND THEORY

Before the system model can be developed it is necessary to establish a background in several areas. In order of discussion these areas are: the phenomenon of "speckle," the forms of the Huygens-Fresnel integral, the use of statistics in modeling, and the process of detection.

Speckle

When the image of an object is produced either through direct detection or heterodyne detection, a random interference pattern also results which breaks up and distorts the desired image. This random interference pattern has been named "speckle" and is the result of the roughness of most object surfaces compared to the wavelength of the incident radiation. Of course, the radiation must be coherent to observe an interference pattern. The most obvious example of speckle is the direct observation of the pattern produced at a rough surface that is being illuminated by a visible laser. This phenomenon was first noted in the early 1960's by Oliver (Ref 1:220) and by Rigden and Gordon (Ref 2:2367-2368). The use of the term "speckle" has grown to include any random diffraction pattern which disrupts the coherent properties of some form of radiation. Speckle occurs in many different circumstances, including rough surface scattering, atmospheric transmission, and holography. Much information covering the different areas of the subject is now available including a complete Journal of the Optical

Society of America volume (Ref 3) and a book edited by Dainty (Ref 4). Dainty also includes a good introduction that briefly covers the history of speckle related phenomena. Also the theory of the scattering of electromagnetic waves from rough surfaces is excellently described in a book by Beckman (Ref 5). Goodman has specialized much of this information for the case of optical intensity radiation (Ref 4: Chapter 2, 16:1688-1700). The major concern in this thesis, however, will be for the case of the direct measurement of optical fields.

Huygens-Fresnel Integral

The real scalar optical field, $u(\bar{r},t)$, is in general a function of time, t, and space, $\bar{r}$, where $\bar{r}$ is a vector with Cartesion components (x,y,z). A temporally modulated field located about frequency, f_o, can be written as

$$\begin{aligned} u(\bar{r},t) &= A(\bar{r},t)\cos[2\pi f_o t + \phi(\bar{r},t)] \\ &= \mathrm{Re}\{A(\bar{r},t)\exp[-j\phi(\bar{r},t)]\exp[-j2\pi f_o t]\} \\ &= \mathrm{Re}\{U(\bar{r},t)\exp[-j2\pi f_o t]\} \end{aligned} \tag{1}$$

where $\mathrm{Re}\{\cdot\}$ is the real operator and $U(\bar{r},t)$ is the complex envelope of the complex representation of $u(\bar{r},t)$. The temporal Fourier transform of $u(\bar{r},t)$ is

$$\begin{aligned} F_t[u(\bar{r},t)] &= \tfrac{1}{2}F_t[U(\bar{r},t)e^{-j2\pi f_o t}] \\ &\quad + \tfrac{1}{2}F_t[U^*(\bar{r},t)e^{j2\pi f_o t}] \end{aligned} \tag{2}$$

where $F_t[g(t)] = \int_{-\infty}^{\infty} g(t)\exp[-j2\pi f\, t]dt$ and the asterisk, (*),

represents the conjugation process. From a graphical representation of Eq. (2), shown in Fig. 2, it can be seen that the transforms of $U(\bar{r},t)$ and $U^*(\bar{r},t)$ are centered at the minus and plus frequencies of f_o respectively. If $u(\bar{r},t)$

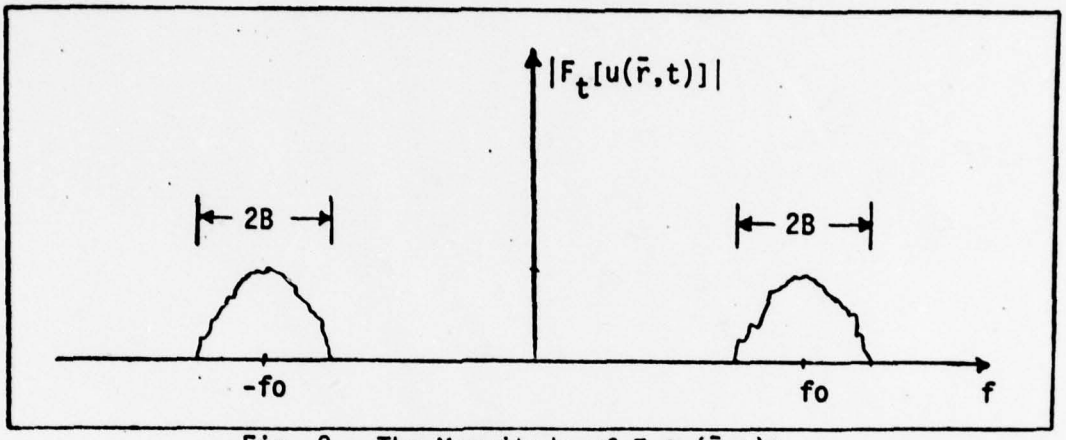


Fig. 2. The Magnitude of $F_t[u(\bar{r},t)]$

is unmodulated the complex envelope equals $U(\bar{r})$ and the Fourier transform becomes two Dirac delta functions that are located only at frequencies plus and minus f_o. This field is then called monochromatic because of the one frequency component. If $u(\bar{r},t)$ is modulated, i.e., time varying amplitude or phase as represented in Fig. 2, then the field is called quasimonochromatic provided the bandwidth, B, of $F_t[U(\bar{r},t)]$ is much less than f_o, i.e., $B<<f_o$. Thus for either monochromatic or quasimonochromatic fields the complex envelope of $u(\bar{r},t)$ can be used to represent the field and the real field can be obtained through Eq. (1). Therefore, throughout most of this thesis, the complex envelope will be used and the expontential optical time function suppressed. In addition, the field is often described

at a particular z plane so that the field varies only in x and y. Thus, the unmodulated optical time varying field at a z plane can be described through the complex envelope, $U(x,y)$.

As shown by Goodman (Ref 7:58), the complex envelope of a monochromatic field at a point in one plane can be expressed in terms of the complex envelope of a field at another plane through the following Huygens-Fresnel integral equation:

$$U(x,y) = \iint_{\Sigma} \frac{1}{j\lambda r_{01}} \exp[jkr_{01}]\cos(\bar{n},\bar{r}_{01})U(\alpha,\beta)d\alpha d\beta \qquad (3)$$

The vector $\bar{r}_{01}$ is shown in Fig. 3, k is the magnitude of the propagation vector which is equal to $2\pi/\lambda$, λ is the optical wavelength, and $\cos(\bar{n},\bar{r}_{01})$ is the cosine of the angle between $\bar{r}_{01}$ and the normal to the α,β plane. Eq. (3) can be simplified through several approximations. If the angle between $\bar{n}$ and $\bar{r}_{01}$ is limited to less than 18^{o} then the $\cos(\bar{n},\bar{r}_{01})$ is approximately equal to one. The integral over the aperture, Σ, can be replaced by an integral of infinite limits if the finite extent of the field, $U(\alpha,\beta)$, due the aperture is included in the mathematical description of $U(\alpha,\beta)$. In addition, if the distance z is much greater than the maximum linear distance from the z axis, then r_{01} in the denominator can be approximated by z. The above restrictions have put the integral in a simpler form and are discussed in greater detail by Goodman,

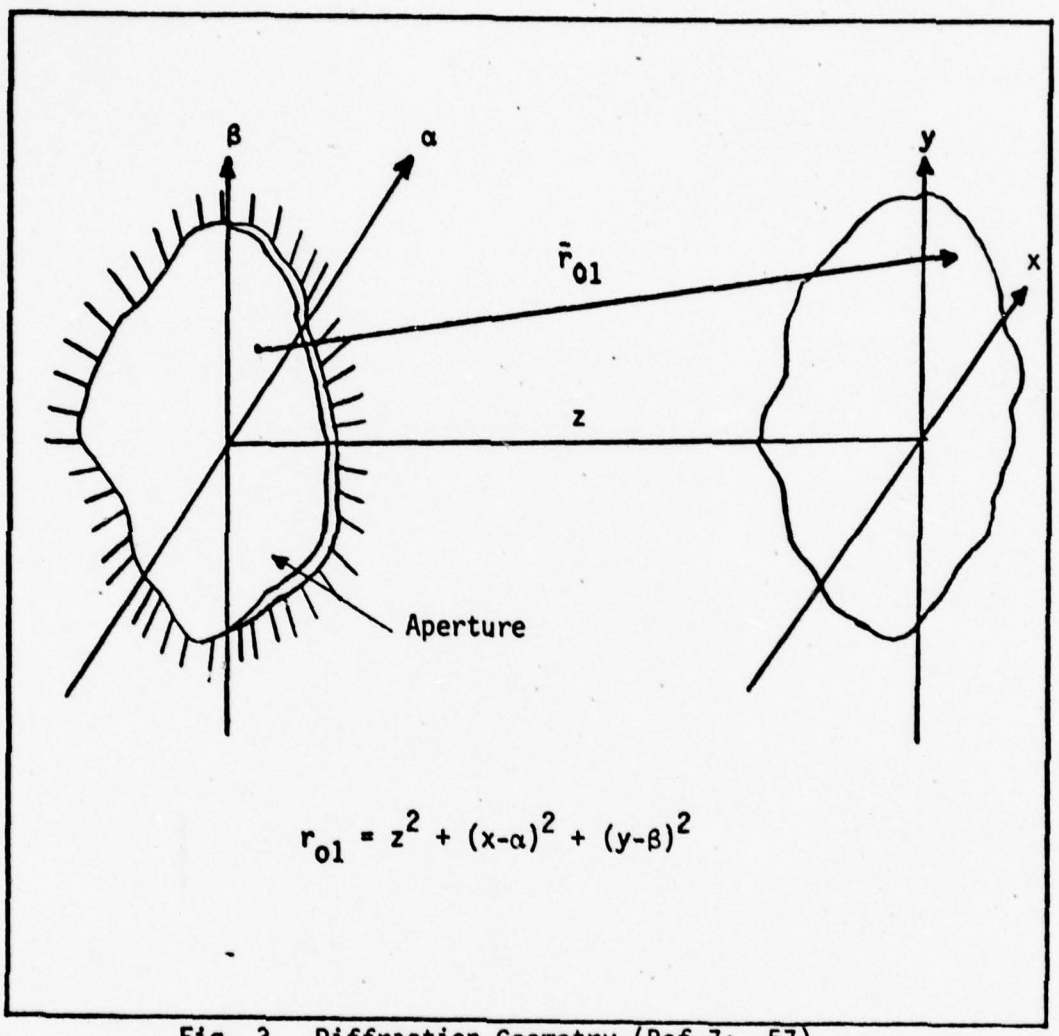


Fig. 3. Diffraction Geometry (Ref 7: 57)

(Ref 7:58). The integral now becomes:

$$U(x,y) = \frac{1}{j\lambda z} \int_{-\infty}^{\infty} U(\alpha,\beta)\exp[jkr_{01}]d\alpha d\beta \qquad (4)$$

The integral is still not very useful because of the r_{01} term in the exponential. But, because the exponential is very sensitive to small changes in the value of exponent, extra care must be used in making any approximations in the

exponential. The two approximations commonly made at this point are the Fresnel and Fraunhofer approximations.

Fresnel Approximation. The Fresnel approximation is made by writing r_{01} from Fig. 1 as:

$$r_{01} - [z^2+(\alpha-x)^2+(\beta-y)^2]^{1/2} \approx z[1+(\frac{\alpha-x}{z})^2+(\frac{\beta-y}{z})^2]^{1/2} \qquad (5)$$

Since the absolute value of the difference terms divided by z is less than one, the binomial expansion to the square root can now be used to write:

$$r_{01} = z[1+\frac{1}{2}(\frac{\alpha-x}{z})^2 + \frac{1}{2}(\frac{\beta-y}{z})^2 - \frac{1}{8}(\frac{\alpha-x}{z})^4 + \cdots\cdots] \qquad (6)$$

Now if the maximum linear distance is such that

$$z^3 >> \frac{\pi}{4\lambda}[(\alpha-x)^2 + (\beta-y)^2]^2_{max} \qquad (7)$$

then the higher order terms beyond the squared terms may be neglected and Eq. (4) reduces to the Fresnel approximation given as:

$$U(x,y) = \frac{\exp[jkz]}{j\lambda z} \iint_{-\infty}^{\infty} U(\alpha,\beta)\exp[\frac{jk}{2z}[(\alpha-x)^2 + (\beta-y)^2]]d\alpha d\beta \qquad (8)$$

or

$$U(x,y) = \frac{\exp[jkz]\exp[\frac{jk}{2z}(x^2+y^2)}{j\lambda z} \iint_{-\infty}^{\infty} U(\alpha,\beta)[\exp\frac{jk}{2z}(\alpha^2+\beta^2)] \exp[\frac{-j2\pi}{\lambda z}(x\alpha+y\beta)]d\alpha d\beta \qquad (9)$$

Fraunhofer Approximation. The Fraunhofer approximation is used when:

$$z >> \left.\frac{k(\alpha^2+\beta^2)}{2}\right|_{max} \tag{10}$$

If Eq. (10) holds, then the squared phase terms may be neglected in the integral of Eq. (9) and the Fraunhofer approximation is written as:

$$U(x,y) = \frac{\exp[jkz]\exp[\frac{jk}{2z}(x^2+y^2)]}{j\lambda z} \int\int_{-\infty}^{\infty} U(\alpha,\beta)$$

$$\exp[\frac{-j2\pi}{\lambda z}(x\alpha + y\beta)]d\alpha d\beta \tag{11}$$

The integral in Eq. (11) can now be recognized as the two dimensional Fourier transform of $U(\alpha,\beta)$ evaluted at the spatial frequencies $f_x = \frac{x}{\lambda z}$ and $f_y = \frac{y}{\lambda z}$.

<u>One-Dimensional Huygens-Fresnel Integral</u>. In many cases the effect of the basic parameters in a system can be adequately described in simpler terms through the use of the one-dimensional Huygens-Fresnel intergral. In this case the field at the z plane is variable in only one lateral direction. The integral is now written as (Ref 22:316):

$$U(x) = \frac{\exp[j(kz-\frac{\pi}{4})]\exp[jk\frac{x^2}{2z}]}{(\lambda z)^{1/2}} \int\int_{-\infty}^{\infty} U(\alpha)\exp[\frac{jk\alpha^2}{2z}]$$

$$\exp[-j2\pi\frac{x\alpha}{\lambda z}]d\alpha \tag{12}$$

Up until this point it has been implied that the Huygens-Fresnel integral can be used only for monochromatic waves. However, the integral may be used for quasimonochromatic waves provided $\frac{1}{B} >> \frac{|\bar{r}_{01}|_{max}}{c}$ where c is the speed of light (Ref 7:108). B is the bandwidth of the complex envelope as shown in Fig. 2.

Propagation and Reflection of a Laser Beam. When Eq. (11) is used to propagate the output from a laser source the result is a Gaussian spherical wave (Ref 8:306) of the following form

$$U(\alpha,\beta) = A \exp[jkz]\exp[j\frac{k}{2z}(\alpha^2+\beta^2)]\exp[\frac{\alpha^2+\beta^2}{w^2(z)}] \qquad (13)$$

where A is an amplitude term . The beam spot size at the z plane, w(z), is the radial distance where the total beam amplitude is e^{-1} times the center amplitude. If it is now desired to reflect this wave directly back from normal incidence on a smooth surface using the same coordinate system, then the exponential phase terms must be conjugated. By conjugating the exp[jkz] term, the wave now propagates in the oposite direction, and by conjugating the $\exp[j\frac{k}{2z}(\alpha^2+\beta^2)]$ term, the spherical phase fronts are inverted. The inversion of the wavefront can be seen by simply drawing rays and then reconstructing the wavefront. More formally the spherical wave can be broken up into an infinite sum of plane waves of different angles of incidence. The surface boundary conditions can be applied to each plane wave and the resulting sum then used to reform the reflected spherical wave. In addition, since a wave is seldom totally reflected, a reflection coefficient, a (α,β), that is a real function of the particular surface must be multiplied times the incident field to complete the process of reflection, (Ref 9:74). In general the reflection coefficient depends on the incident angle and polarization of the

incident field and on the index of refraction of the surface. The reflected field is modeled as

$$U_r(\alpha,\beta) = a\ (\alpha,\beta)U_i^*(\alpha,\beta) \qquad (14)$$

where r denotes the reflected wave and i denotes the incident wave

Statistics in Modeling

In many instances the exact nature of the desired signal field is unknown either because the signal itself is unknown or because a known signal has been distorted by some type of unknown interference, or both. In these cases it is useful to model the system through the use of statistics.

In statistics a random variable is an unknown function, x, whose possible values are best described by a probability density function (Ref 10:92-136). Each possible value of x is called a sample point. In many cases x is also a function of time, termperature, space, or any other index and is then called a random process (Ref 10:298-339). Thus a random process is a collection of random variables that are indexed by another parameter so the probability density also becomes a function of the index. For any particular value of the index, (x) is a random variable. For any fixed value (sample) of a random variable (x) is still a function of the index and is called a sample function. To describe the random process completely, all orders of the combined

probability densities for all possible values of the index must be known (Ref 10:311). But, in practice this requires more knowledge of the random process than is usually available. Therefore a limited statistical description of the system, called a second moment model, is commonly used. The mean, variance, correlation, and covariance function are used in a second moment analysis.

The mean of a random process, x, is in general a function of the index, t, and is denoted as $E[x_t]$ where $E[\cdot]$ is the expected value operator (Ref 10:Chapter 7). The mean is the first moment of the process and is often called the expected value of the process or the ensemble average. The mean crudely represents the "most likely" sample function of the random process and is usually directly related to the desired signal. The variance describes the average of the square of the fluctuations about the mean and is defined by (Ref 10:244)

$$\sigma_x^2(t) = E[(x_t - E[x_t])^2] = E[x_t^2] - E^2[x_t] \qquad (15)$$

where again the index, t, has been included because x is a random process. The variance is usually considered an indication of "noise" in the system because it is a measure of the variation or fluctuations of the random process from the desired mean term. The square root of the variance is usually denoted as the standard deviation or the rms variation from the mean.

Since the process varies with the index, the mean and variance are not sufficient information to describe how the process is related to itself at different values of the index. This relationship is described to some degree through the correlation (or autocorrelation) and covariance functions. The covariance function is defined as (Ref 10: 317)

$$C_x(t_1,t_2) = E[(x_{t_1}-E[x_{t_1}])(x_{t_2}-E[x_{t_2}])$$

$$= E[x_{t_1} x_{t_2}] - E[x_{t_1}]E[x_{t_2}]$$

$$= R_x(t_1,t_2) - E[x_{t_1}]E[x_{t_2}] \qquad (16)$$

where $R_x(t_1,t_2)$ is called the correlation function. If $t_1=t_2$ then the covariance is equal to the variance and if the mean is zero, the covariance is equal to the correlation function.

Because the covariance depends on the individual values of the index, it may still require more information than is usually known. But, in some cases the statistics can be considered stationary at least at the second moment level (Ref 10:325). Under this condition the mean becomes a constant (independent of the index) and the covariance and correlation functions depend only on the absolute difference in the index values, $t_2-t_1=\Delta t=\tau$. This assumption may appear invalid for a particular random process, but it only means that the process is being described by a rather crude but still useful set of statistics. Under the condi-

tion of stationarity, Eq. (16) now becomes:

$$c_x(\tau) = R_x(\tau) - E^2[x] \tag{17}$$

The covariance and correlation functions of a real random process can be shown to be even functions of τ with their maximum magnitude at $\tau=0$ (Ref 10:323). Also, for a nonperiodic process, the correlation function approaches the square of the mean and the covariance approaches zero as τ approaches infinity. In many cases the effective non-zero value of the covariance occurs over just a short length of τ from the origin. This period of τ is called the correlation or coherence period (time, distance), τ_c, of the random process. Although the exact point at which the covariance can be considered to be zero for a particular function may be rather arbitrary, τ_c roughly represents the distance (or time separation) between samples of the process such that the samples become unrelated i.e., uncorrelated. A typical sample function with statistical parameters crudely identified is shown in Fig. 4a. A sample correlation function is shown in Fig. 4b.

Measurement of Optical Signals

To retrieve the information from an optical signal, there must be some means of measurement. Most available optical detectors are square law devices that measure the intensity of the incident field, i.e. $|u(x,y)|^2$ (Ref 11:1819). However, homodyne and heterodyne techniques can be used to measure the actual field with its accompanying phase

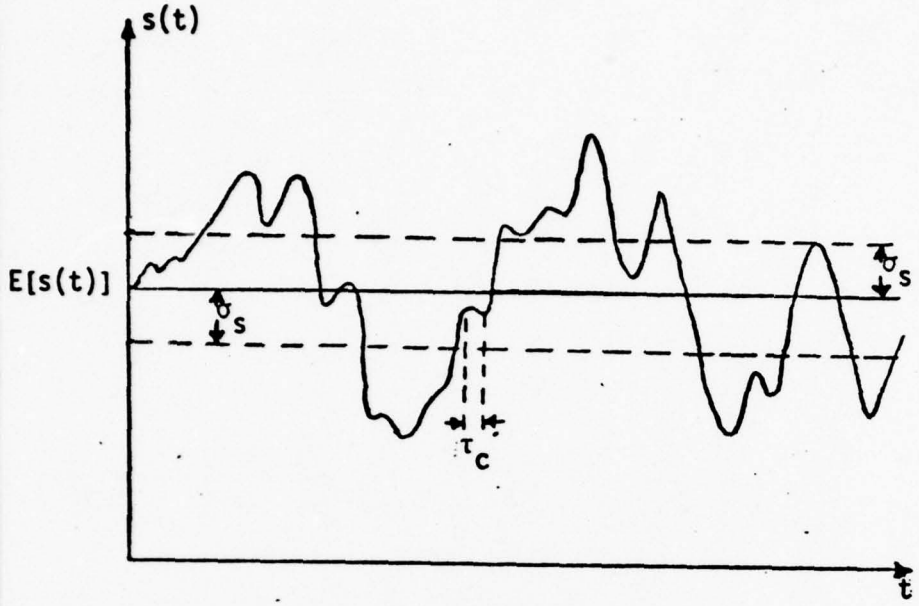


Fig. 4a Sample Function

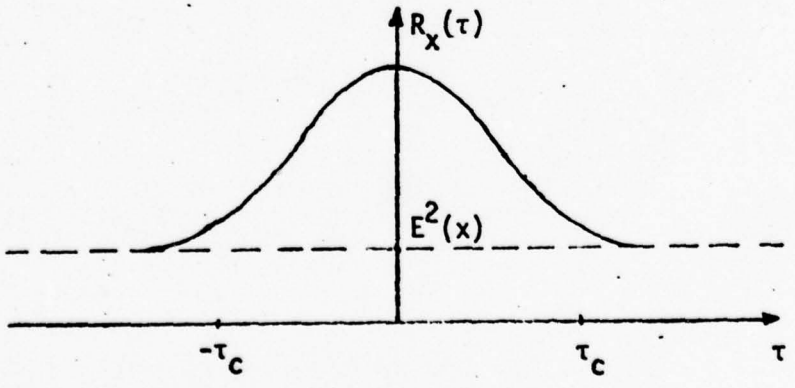


Fig. 4b A Correlation Function

Fig. 4 Illustrations of Typical Statistical Relationships

information. While the system to be discussed in this thesis is a heterodyne system, a brief discussion of direct detection will be given first so that the difference in the necessary field statistics can be related. The detectors considered here will be modeled as ideal, i.e., all quantum effects and noise terms will be neglected. This will allow the speckle noise term to be isolated in this thesis. The detector noise terms can always be added to the model if it becomes necessary.

Direct Detection. The ideal instantaneous output of an optical detector is defined as (Ref 12:91)

$$i(t) = \frac{q\eta}{hf_o} P_c = \frac{q\eta}{hfo} \iint_{A_d} |U_s(x,y)|^2 dxdy \tag{18}$$

where q is the charge of an electron

η is the quantum efficiency of the detector

h is the Planck's constant

f_o is the optical frequency

P_c is the optical power collected by the detector surface

A_d is the area of the detector surface

$U_s(x,y)$ is the signal field incident on the detector.

Thus this sytem directly measures the intensity of the field and is referred to as direct detection.

The mean current is

$$E[i(t)] = \frac{q\eta}{hfo} \iint_{A_d} E[U_s(x,y)U_s^*(x,y)]dxdy \tag{19}$$

where the asterisk denotes the complex conjugate of the field. Therefore the expected value of the current is related to the expected value of the intensity of the field or the correlation function of the field. Similarly the correlation function of the current is related to a fourth order moment of the field as shown below:

$$E[i(t)i(t')] = \left(\frac{q\eta}{hfo}\right)^2 \iiiint_{A_d} E[U_s(x,y)U_s^*(x,y)U_s(x',y')U_s^*(x',y')]dxdydx'dy' \quad (20)$$

Heterodyne Detection. In a heterodyne system the incoming signal field is added to a local oscillator field, $U_{LO}(x,y,t)$, by means of a beam splitter. The local oscillator field is at an optical frequency of $f_o - f_{IF}$. With this arrangement the ideal detector output current becomes (Ref 13:481-487)

$$\begin{aligned} i(t) &= \frac{q\eta}{hfo} \iint_{A_d} |U_s(x,y,t) + U_{LO}(x,y,t)|^2 dxdy \\ &= \frac{q\eta}{hfo} \iint_{A_d} \{|U_s(x,y)|^2 + 2Re[U_s(x,y)U_{LO}^*(x,y)\exp[-j2\pi f_{IF}t]] \\ &\quad + |U_{LO}(x,y)|^2\}dxdy \end{aligned} \quad (21)$$

where $Re[\cdot]$ is the real operator. The first and last terms in the integral are centered at zero frequency and can be filtered out so that the remaining output is at the intermediate frequency, f_{IF}, as shown below

$$i(t) = \frac{2q\eta}{hfo} \iint_{A_d} Re\{U_s(x,y)U_{LO}^*(x,y)\exp[-j2\pi f_{IF}t]\}dxdy \quad (22)$$

Since the expected value and real operator are both linear they can be interchanged and, assuming that the signal field is the only random quantity, the expected value of the current is:

$$E[i(t)] = \frac{2q\eta}{hf_o} \iint_{A_d} \mathrm{Re}\{E[U_s(x,y)]U_{LO}^*(x,y)\exp[-2j\pi f_{IF}t]\}dxdy \quad (23)$$

Thus for heterodyne detection the mean of the current is related to the mean of the field. This is in contrast to the case of direct detection where the mean of the current from Eq. (19) is proportional to the correlation of the field, i.e., $E[U_s(x,y)U_s^*(x,y)]$. The correlation function of the current for heterodyne detection is:

$$\begin{aligned} E[i(t)i(t')] &= \left(\frac{2q\eta}{hf_o}\right)^2 E\Big[\iiiint_{A_d} \mathrm{Re}[U_s(x,y)U_{LO}^*(x,y) \\ &\quad \exp[-j2\pi f_{IF}t\,]\mathrm{Re}[U_s(x',y')U_{LO}^*(x',y') \\ &\quad \exp[-\,j2\pi f_{IF}t']dxdydx'dy' \\ &= \left(\frac{2q\eta}{hf_o}\right)^2 \mathrm{Re}\Big\{\iiiint_{A_d} E[U_s(x,y)U_s(x',y')]U_{LO}^*(x,y) \\ &\quad U_{LO}^*(x',y')\exp[-j2\pi f_{IF}(t+t')]+E[U_s(x,y) \\ &\quad U_s^*(x',y')]U_{LO}^*(x,y)U_{LO}(x',y')\exp[-j2\pi f_{IF} \\ &\quad (t-t')]dxdydx'dy'\Big\} \end{aligned} \quad (24)$$

where identity $\mathrm{Re}[A]\mathrm{Re}[B] = \mathrm{Re}[AB+AB^*]$ has been used. Therefore in heterodyne detection the correlation of the current is related to the correlation of the real parts of the field and is in general nonstationary.

The discussion of the background theory is now complete. The task is to now use these models and ideas that have been presented in this section to develop a complete system model for the heterodyne line-scan imaging system.

III. THE SYSTEM MODEL

Now that the background theory has been discussed the system model can be developed. First a phase model for the rough surface will be established, then this phase model will be incorporated into the total heterodyne line-scan imagery model. From the system model the mean and covariance functions of the complex output current will be determined. For simplicity the model will be developed in one dimension as explained later.

The Rough Surface Phase Model

The reflection from a rough surface is in general a very complicated process that involves the surface reflection coefficients, the surface height variations, the macroscopic and microscopic angles of incidence, and the polarization of the incident field. Since the system discussed here involves the imaging of many different types of surfaces with characteristics beyond the system's control, and since the usable information is only in the direct backscattered radiation, a more simple phenomelogical model will be used. The model, which was also used in a similar direct detection imaging problem (Ref 14:779-785), is less complicated than Beckman's (Ref 5:Chapter 5) but is closely related. The model will be developed under the following conditions: (1) scalar fields will be used, (2) depolarization effects, multiple scattering, and shadowing will be neglected, as is typically the case (Ref 5:Chapter 3 and 5,

6:1689) since the effects are often small and very difficult to describe mathematically, (3) the surface will be considered rough as compared to the optical wavelength as discussed in more detail later so that backscattered radiation exists and total specular reflection does not occur, (4) the radius of curvature of the surface irregularities will be assumed large as compared to the optical wavelength (Ref 5:20), and (5) the field reflectivity will be considered a real function of space with a value between zero and one so that it attenuates the incident field such that the reflectivity is the surface characteristic to be measured, i.e. the signal.

Under the above conditions the reflection from a rough surface will be modeled by including a random phase term in the process of reflection from a smooth surface given by Eq. (14) in the background section. The reflected wave is then:

$$U_r(\alpha) = a(\alpha)e^{j\theta(\alpha)}U_i^*(\alpha) \qquad (25)$$

The random phase can now be related to the surface heights. First, the surface heights, $h(\alpha)$, will be modeled as a stationary zero mean Gaussian random process. The zero mean follows from the fact that any constant reference can be added to the model such that the ensemble average becomes zero. A Gaussian distribution is commonly used to describe a rough surface (Ref 4:65, 3:1153, 1195, 1205, 1212, 1224, 5:80) but may break down for some polished man made surfaces.

As will be discussed later this is not a particularly necessary assumption, but it does make the problem easier mathematically.

As can be seen from the sample function of Fig. 5, the total path difference between a wave reflected at h(α) and a wave reflected at h(o) referenced to a constant spherical phase front is

$$\Delta r = d+\frac{k\alpha^2}{2z} - h(\alpha)+d-\frac{k\alpha^2}{2z} - h(\alpha)-d-\frac{k\alpha^2}{2z}-d+\frac{k\alpha^2}{2z}=-2h(\alpha) \quad (26)$$

an so the phase variation becomes:

$$\theta(\alpha) = \frac{2\pi}{\lambda}(2h(\alpha)) = \frac{4\pi}{\lambda} h(\alpha) \quad (27)$$

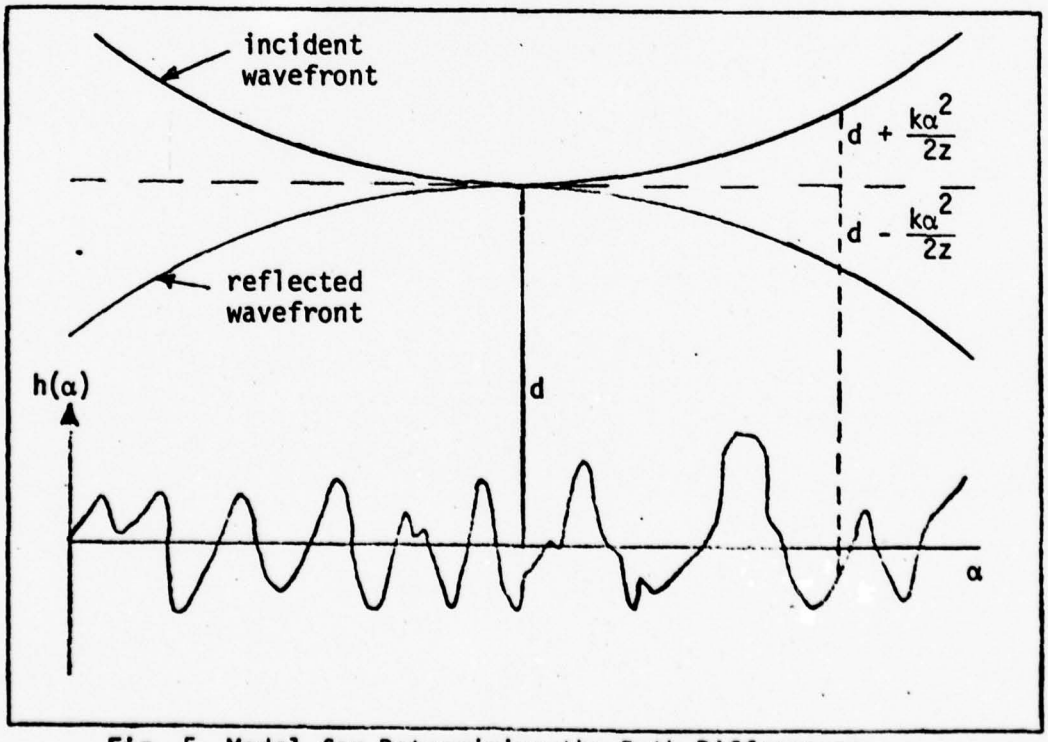


Fig. 5 Model for Determining the Path Differences Induced by the Rough Surface

The mean of the phase is

$$E[\theta(\alpha)] = \frac{4\pi}{\lambda} E[h(\alpha)] = 0 \tag{28}$$

and the variance of the phase is:

$$\sigma_\theta^2 = \left(\frac{4\pi}{\lambda}\right)^2 \sigma_h^2 = \left(\frac{4\pi\sigma_h}{\lambda}\right)^2 \tag{29}$$

From Eq. (29) it can be seen that the rms roughness of the surface, σ_h, can be directly compared to the wavelength, λ. When the wavelength is large compared to σ_h, the rms variation of the phase is small and there would be little problem with interference. But, as σ_h approaches the value of λ or greater, the rms phase variations become larger than 2π radians, and destructive interference will result. An example of some values of rms surface roughness is shown in Table 1. Most exterior metal surfaces will fall in the

Table I Values of Surface Roughness

Name	rms roughness		average peak to peak height	
	micro-inches	microns	micro-inches	microns
Rough	1000	25.4	3500	88.9
Semirough	500	12.7	1750	44.45
Medium	250	6.35	875	22.2
Semifine	125	3.18	455	11.56

(From Ref. 15:859)

category of rough to semirough and thus would also be considered rough as compared to an optical wavelength. Also most other nonmetalic surfaces are rough compared to metal surfaces so they, too, would be rough compared to an optical wavelength.

Later in determining the moments of the fields it will be necessary to take the expected value of the random exponential phase terms as follows:

$$E[e^{j\theta}] \tag{30}$$

$$E[e^{j[\theta(\alpha)-\theta(\alpha')]}]=E[e^{j\phi}] \tag{31}$$

and

$$E[e^{j[\theta(\alpha)+\theta(\alpha')]}] = E[e^{j\gamma}] \tag{32}$$

The above two equations represent a form of the characteristic function (Ref 10:419)

$$\phi_x(v) = E[e^{jvx}] \tag{33}$$

for the case of v=1. For a Gaussian random variable, x, the characteristic function is well known and equals (Ref 10:420):

$$\phi_x(v) = \exp[jvE[x] - \frac{v^2\sigma_x^2}{2}] \tag{34}$$

Thus, for Eqs (30), (31) and (32), v=1 and the mean is zero so the characteristic function equals:

$$E[e^{j\psi}] = e^{\frac{-\sigma_\psi^2}{2}} \tag{35}$$

where $\psi=\theta,\phi$, or γ as required. The variance of θ was determined in Eq. (29). For a stationary zero mean

Gaussian random process the variance of ϕ is computed as follows:

$$\begin{aligned}\sigma_\phi^2 &= E[(\theta(\alpha)-\theta(\alpha'))^2]-E^2[\theta(\alpha)-\theta(\alpha')] \\ &= E[\theta^2(\alpha)+\theta^2(\alpha')-2\theta(\alpha)\theta(\alpha')] \\ &= 2\sigma_\theta^2 - 2R_\theta(\Delta\alpha) \\ &= 2\sigma_\theta^2(1-\rho(\Delta\alpha)) \end{aligned} \tag{36}$$

where $\Delta\alpha=\alpha-\alpha'$ and $\rho(\Delta\alpha)$ is the correlation function of the phase normalized to one at $\Delta\alpha=0$. $\rho(\Delta\alpha)$ is also identically the normalized correlation function of the surface heights, $h(\alpha)$. Similarly

$$\sigma_\gamma^2 = 2\sigma_\theta^2(1+\rho(\Delta\alpha)) \tag{37}$$

The Heterodyne Detector Current Model

The rough surface model is now complete and must be incorporated into the system model. The output field from the illuminating laser will be propagated to a rough surface, reflected, and propagated back to the detector by means of the Huygens-Fresnel integral equation. The detector current will be determined from this field. Then the statistical moments of the current will be determined and it will be shown that the system can be described in terms of the complex current output of the detector.

The Real Current. The mechanics of the heterodyne line-scan system scan the laser radiation across the scene to be

imaged and the detector measures the backscattered field. The system mechanics also keeps the detector surface and local oscillator field aligned normal to the direction the laser is pointing. However, the angle of incidence between the laser field and the object surface will change as the beam is swept across the object. In principle the coordinate rotations required to describe this scanning system could all be included in the Huygens-Fresnel integral but the problem becomes more complicated than useful. Therefore, the system will be modeled with the laser, detector, and associated fields in a fixed coordinate system. The laser beam will be normally incident upon an object surface whose reflectivity and random phase characteristics are effectively moving beneath the beam in time and with velocity, V. Both the spreading of the beam spot and the changing surface velocity that occur as the beam is swept over the surface will be ignored. But, the model will be a function of the beam width and the velocity so the above effects can be determined simply by varying these parameters. Also, at any instant of time, the detector output is proportional to an average of all the reflectance values at each point within the beam spot and detector field of view. Because the laser beam is circular in shape, the reflectance points covered by the width of the beam at each point in the scanning direction will change slightly as the beam is moved. But, the basic change in the average reflectance is caused

by the reflectance points that enter and leave the beam in the scanning direction. Thus the model will be developed in the scanning direction only, where the reflectance at each point in this direction can be thought of as an average of the reflectance over the width of the beam. The extension of the model to both lateral dimensions is straightforward but more tedious.

The system geometry is shown in Fig. 6. From Eqs (12)

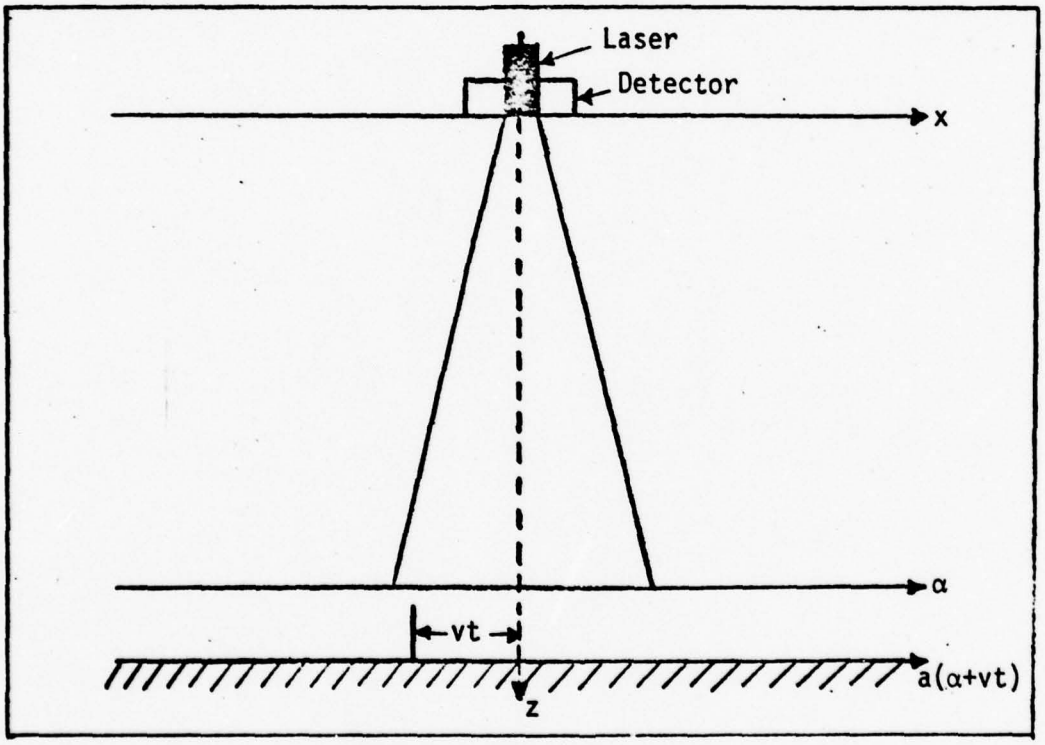


Fig. 6 System Geometry

and (13) the one dimensional field from the laser at the object surface is:

$$U_i(\alpha) = \frac{\exp[j(kz-\frac{\Pi}{4})]}{(\lambda z)^{1/2}} A \exp[-(\frac{\alpha}{w(z)})^2]\exp[j\frac{k\alpha^2}{2z}] \qquad (38)$$

From Eq. (25) where the reflectivity and random phase are now properties of a moving surface, the backscattered field is:

$$U_r(\alpha) = a(\alpha-vt)e^{j\theta(\alpha-vt)} U_i^*(\alpha) \qquad (39)$$

The reflected field is now propagated back to the detector through the Huygens-Fresnel integral of Eq. (12) but since propagation is now in the negative z direction the phase terms of the Huygens-Fresnel integral of Eq. (12) must also be conjugated so that the field at the detector is

$$U_d(\alpha) = \frac{\exp[-j(kz-\frac{\Pi}{4})]\exp[-jk\frac{x^2}{2z}]}{(\lambda z)^{1/2}} \int_{-\infty}^{\infty} U_r(\alpha)\exp[-j\frac{k\alpha^2}{2z}]$$

$$\exp[j2\Pi\frac{x\alpha}{\lambda z}]d\alpha \qquad (40)$$

From substituting Eqs. (38, 39, and 40) into Eq. (22) the detector output current becomes

$$i_r(t) = \frac{2q\eta A}{hf_o\lambda z} \mathrm{Re}\{\exp[-j2(kz-\frac{\Pi}{4})] \int\int_{-\infty}^{\infty} P_D(x)a_o(\alpha+vt)$$

$$\exp[(\frac{\alpha}{w(z)})^2]\exp[j\theta(\alpha+vt)]\exp[-j\frac{k\alpha^2}{z}]\exp[-j\frac{kx^2}{2z}]$$

$$\exp[j2\Pi\frac{x\alpha}{\lambda z}]U_{LO}^*(x)\exp[-j2\Pi f_{IF}t]dxd\alpha\} \qquad (41)$$

where $P_D(x)$ is the limiting detector aperture function. A simplication to Eq. (41) can be made by realizing that $P_D(x)$ can represent a lens aperture and transfer function

or just the detector aperture size. If the local oscillator field is a plane wave the x integral in the above equation yields the Fresnel diffraction pattern of $P_D(x)$. However, this can be simplified by realizing that in most cases $P_D(x)$ is narrow enough to satisfy the Fraunhofer type approximation given by Eq. (10). If this is not the case the $\exp[-j\frac{kx^2}{2z}]$ phase term can still be negated either by a conjugate lens transfer function (converging lens) or by an identical phase term from the local oscillator field. In any case $U_{LO}(x)$, $\exp[pj\frac{kx^2}{2z}]$, and any phase term in $P_D(x)$ can be all combined to equal one, so that $P_D(x)$ is now just the limiting aperture size. The x integral is now the spatial Fourier transform of $P_D(x)$ evaluated at $f_\alpha = \frac{\alpha}{\lambda z}$. The transform of $P_D(x)$ is denoted as:

$$F_x[P_D(x)]\Big|_{f = \frac{\alpha}{\lambda z}} = P_{DF}(\alpha) \tag{42}$$

Equation (41) now reduces to

$$i_r(t) = BRe\{\exp[-j2(kz-\tfrac{\pi}{4})]\exp[-j2\pi f_{IF}t] \int_{-\infty}^{\infty} h(\alpha)$$

$$\exp[j\theta(\alpha+vt)]\ a(\alpha+vt)\exp[-j\tfrac{k\alpha^2}{z}]d\alpha\} \tag{43}$$

where $B = \frac{2q\eta A}{hf_o\lambda z}$

and $$h(\alpha) = P_{DF}(\alpha)\exp[-(\tfrac{\alpha}{w(z)})^2]. \tag{44}$$

$h(\alpha)$ will be referred to as the system function and represents the combined result of the beam spot size and the detector field of view.

The Complex Current. As was seen in Eqs. (23) and (24) the moments of the current could be obtained by taking the real part of the moments of the complex current. Thus, the moments of the complex current will now be determined. In determining these moments the phase terms in front of the integral in Eq. (43) can be dropped. It will be shown later that these phase terms are indeed unrelated to the problem solution. Thus the useful complex current is defined as:

$$i(t) = B \int_{-\infty}^{\infty} h(\alpha)a(\alpha+vt)\exp[j\theta(\alpha+vt)]\exp[-j\frac{k\alpha^2}{z}]d\alpha \qquad (45)$$

Since the rough surface phase term is the only random term in Eq. (45) the mean of the current using Eq. (35) is

$$E[i(t)] = B \exp[\frac{-(\sigma_\theta)^2}{2}] \int_{-\infty}^{\infty} h(\alpha)a(\alpha+vt)\exp[-j\frac{k\alpha^2}{z}]d\alpha \qquad (46)$$

where $\exp[\frac{-(\sigma_\theta)^2}{2}]$ is the value of the characteristic function from Eq. (35). The value of the characteristic function for a surface with $\sigma_h \geq \lambda$ in Eq. (29) is 5×10^{-35} or less. For typical values of A=.1, η=1, and $f\lambda=c=3\times10^8$ Eq. (46) becomes (5×10^{-35}) (1.6×10^5) (L/z) where L is the value of the integral in Eq. (46). Since $h(\alpha)$, $a(\alpha+vt)$ and $\exp[\frac{-jk\alpha^2}{z}]$ all are terms with values less than one, L is equal to the beam width or less and thus the mean current is effectively equal to zero.

With a zero mean, the covariance of the current equals the correlation of the current. From Eq (24) the correlation involves the moments: $E[i(t)i(t')]$ and $E[i(t)i^*(t')]$. Using Eq. (45) the first moment is:

$$E[i(t)i(t')] = B^2 \int_{-\infty}^{\infty}\int h(\alpha)h(\alpha')a(\alpha-vt)a(\alpha'-vt')E[\exp\{j[\theta(\alpha-vt)+\theta(\alpha'-vt')]\}]\exp[-j\frac{k}{z}(\alpha^2+\alpha'^2)] \, d\alpha d\alpha' \quad (47)$$

From Eqs. (33, 34, 35, and 37) it is seen that the above expected value term is another characteristic function and is equal to:

$$\phi_\gamma(1) = \exp[-\sigma_\theta^2(1+\rho(\Delta\alpha+v\Delta t))] \quad (48)$$

where $(\alpha-vt)-(\alpha'-vt') \triangleq \Delta\alpha-v\Delta t$. The normalized covariance function of the phase, $\rho(\Delta\alpha+v\Delta t)$, varies between one and zero so that Eqs. (47) and (48) equal zero under the same conditions as for the zero mean current of Eq. (46). The other moment is:

$$E[i(t)i^*(t')] = B^2 \int_{-\infty}^{\infty}\int h(\alpha)h(\alpha')a(\alpha+vt)a(\alpha'+vt')E[\exp\{j[\theta(\alpha+vt)-\theta(\alpha'+vt')]\}]\exp[-j\frac{k}{z}(\alpha^2-\alpha'^2)] \, d\alpha d\alpha' \quad (49)$$

From Eqs. (35) and (36) the above characteristic function is equal to:

$$\phi_{\phi}(1) = \exp[-\sigma_{\theta}^{2}(1-\rho(\Delta\alpha-v\Delta t))] \qquad (50)$$

This function has a value of one for $\Delta\alpha+v\Delta t$ equal to zero and decreases to $\exp(-\sigma_{\theta}^{2})$ as $\Delta\alpha+v\Delta t$ approaches infinity. It can now be seen that the $\exp[-j2(kz-\frac{\Pi}{4})]$ phase term of Eq. (44) is cancelled because of the conjugation of the current in Eq. (49). It also obviously has no effect on the moments that equal zero.

It is necessary to determine a function to describe the normalized covariance function, $\rho(\Delta\alpha)$, with Δt set equal to zero for now. Beckman (Ref 13:81) suggests a Gaussian function of the form

$$\rho(\Delta\alpha) = \exp[-(\frac{\Delta\alpha}{\alpha_{c}})^{2}] \qquad (51)$$

where α_{c} is the correlation distance defined at $\rho(\Delta\alpha)=e^{-1}$. For optically rough surfaces Goodman (Ref 6:1698) points out that α_{c} is generally less than 0.1 mm. Kurtz (Ref 16:984) has shown that when σ_{θ} of Eq. (29) is equal to five or greater the correlation distance of the field at the e^{-1} point is then less than the correlation distance of the rough surface by a factor of $1/\sigma_{\theta}$. Since it has been assumed that σ_{h} of Eq. (29) is greater than a wavelength, then σ_{θ} will be greater than five and the correlation distance of the field through Eq. (50) will be less than $\frac{0.1mm}{5} = .02mm$. Equation (50) will now be called the field correlation pulse function and denoted as $P_{\ell}(\Delta\alpha)$ where ℓ represents the field correlation distance. $P_{\ell}(\Delta\alpha)$ is plotted in Fig. 7 as a

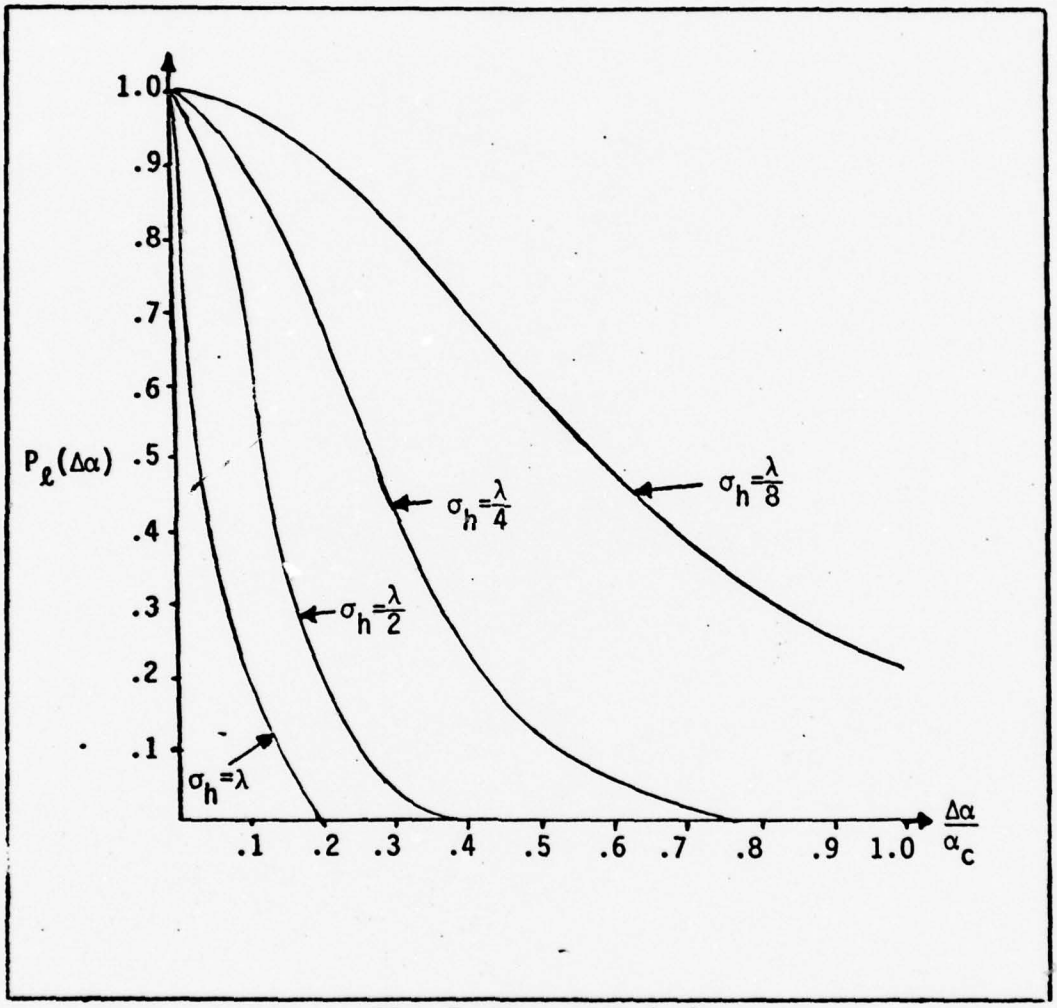


Fig. 7 Plot of $P_\ell(\Delta\alpha)$

function of $\frac{\Delta\alpha}{\alpha_c}$ for several values of σ_h. The plots clearly show that the field correlation distance is less than the surface correlation distance for the case of a rough surface and a Gaussian surface correlation function. However, this result is not strongly dependent on the shape of $\rho(\Delta\alpha)$. Eq. (50) shows that any narrow surface correlation function will cause the field correlation distance, ℓ, to be very small whenever $\sigma_h > \lambda$.

It can be seen by Fig. 8 that $\alpha^2-\alpha'^2$ is greatest when $\alpha-\alpha'$ is at its maximum value. $\alpha-\alpha'$ is now limited by the

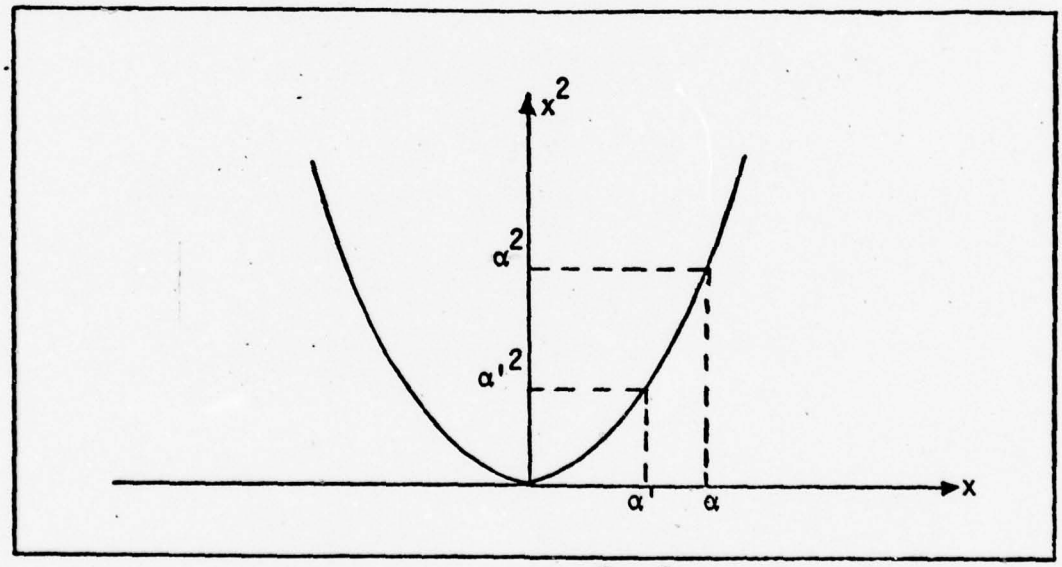


Fig. 8 Comparison of $\alpha^2-\alpha'^2$ to $\alpha-\alpha'$

field correlation distance, ℓ, and α and α' maximum is determined by the beam spot size or the transform of the detector aperture, whichever is less, through the terms; $h(\alpha)$ and $h(\alpha')$. By using the beam spot size $w(z)$ as the limiting term in $h(\alpha)$

$$(\alpha^2-\alpha'^2)\Big|_{max} = w^2(z)-(w(z)-\ell)^2=w(z)\ell-\ell^2\approx w(z)\ell \qquad (52)$$

Now the phase term, $\exp[j\frac{k(\alpha^2-\alpha'^2)}{z}]$, can be approximated by one if:

$$z \gg k(\alpha^2-\alpha'^2)\Big|_{max} = kw(z)\ell \qquad (53)$$

For a beam divergences, $\frac{w(z)}{z}$, of less than three milliradians Eq. (53) will hold. Typically beam divergence is about 1 milliradian, so the approximation given by Eq. (53) appears reasonable. Equation (49) now becomes

$$E[i(t)i^*(t')] = B^2 \int_{-\infty}^{\infty}\int h(\alpha)h(\alpha')a(\alpha+vt)a(\alpha+vt)P_\ell(\Delta\alpha+v\Delta t) \, d\alpha d\alpha' \qquad (54)$$

Equation (54) is identical to the far field case because the quadratic terms no longer affect the result. At t=t' Eq. (54) is the variance of the complex current. The correlation function of Eq. (54) is nonstationary because of the reflectance terms, so the correlation distance is difficult to define. But, an indication of the change in the correlation function as Δt is increased and can be seen by writing Eq. (54) as

$$E[i(t)i^*(t')] = B^2 \int_{-\infty}^{\infty} h(\alpha)a(\alpha+vt)[h(\alpha)a(\alpha+vt')]^*P_\ell (\alpha+v\Delta t)]d\alpha \qquad (55)$$

where * denotes the convolution process.

A graphical picture of Eq. (55) is shown in Fig. 9. The maximum width L of $h(\alpha)a(\alpha+vt)$ and $h(\alpha)a(\alpha+vt')$ is determined

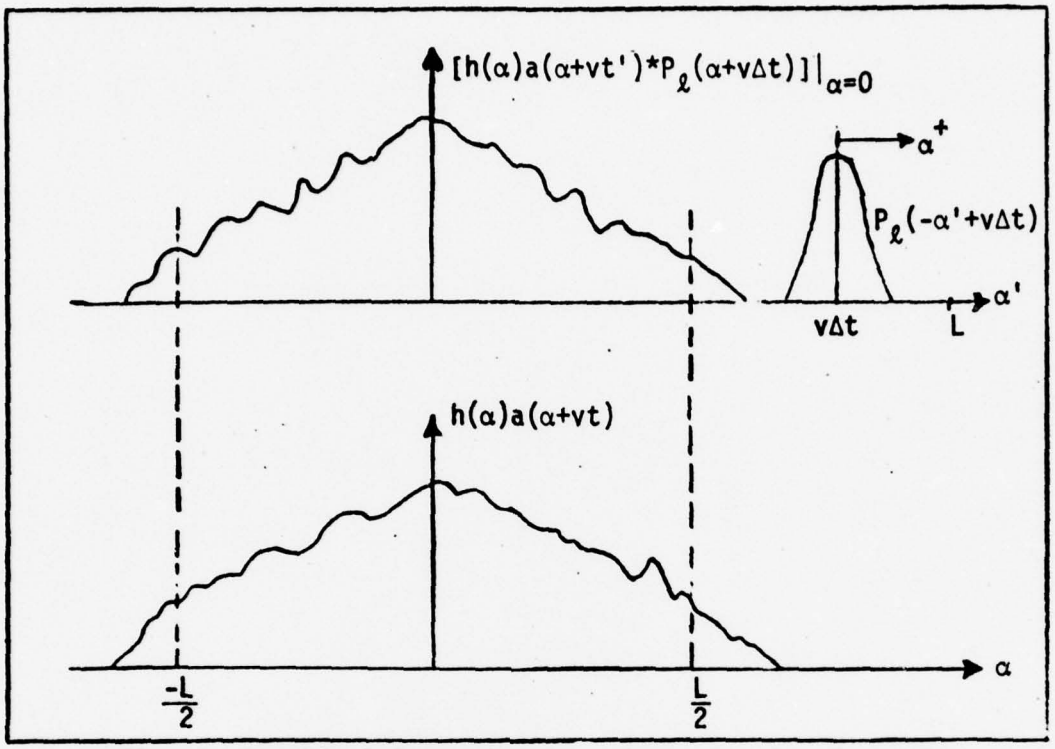


Fig. 9 Graphical Determination of the Complex Current Correlation Distance

by the beam spot size or the Fourier transform of the detector aperture, whichever is less. From Eq. (55) and the figure, the product of $h(\alpha)a(\alpha+vt)$ times the convolution process is zero once $v\Delta t+\ell$ is greater than L. Because the function is nonstationary, this represents a maximum correlation distance and since $\ell \ll L$ the correlation distance is defined as:

$$v\Delta t \triangleq L \tag{56}$$

The above result is rather pleasing since it would seem natural that the output would become uncorrelated once all of the original scattering areas passed out of the system.

From Eq. (56) the correlation time is

$$\Delta t = L/v \tag{57}$$

and the noise bandwidth is approximately:

$$B = \frac{1}{\Delta t} = \frac{v}{L} \tag{58}$$

The results of Eqs. (57) and (58) are similar to those for the case of filtered "white" noise where the correlation time is approximately equal to the response time of the filter and the noise bandwidth is equal to the inverse of the filter response time. However, if the reflectance varies much within the correlation distance given by Eq. (56), then the correlation function will be modulated by the reflectance and the actual correlation distance and time may become less than that given by the above equations. The results presented so far have been based on the commonly used assumption that the surface, and, thus the phase, is a Gaussian random process. This assumption has made the problem mathematically tractible but is not particularly necessary. It has been shown that the characteristic function of several distributions is very small when σ_h is on the order of a wavelength or greater (Ref 14:781). Thus, the mean of the complex current can still be considered equal to zero. Also, the shape of $P_\ell(\Delta\alpha)$ determined as a result of the Gaussian assumption is not critical so long as the correlation distance is still small. This small

field correlation distance is a result of the reflection of a wave from a rough surface. The rough surface by definition is characterized by a short correlation distance. Thus the results presented so far appear to apply to any realistic natural rough surface.

The Signal Detection Models

Since it has been shown from Eq. (46) that the mean of the complex current is zero, it follows that the means of the real and imaginary parts of the current are also zero. Therefore, the mean of the heterodyne detector output current given by Eq. (43) is zero. This does not imply that the mean of the amplitude of the current is zero. The amplitude, A(t), can be identified by writing the complex current as the sum of the real and imaginary parts of the current as follows:

$$i(t) = I_r + jI_i = A(t)\cos\theta(t) + jA(t)\sin\theta(t) \qquad (59)$$

or by writing it in polar from as:

$$i(t) = A(t)e^{j\theta(t)} \qquad (60)$$

The value of the amplitude can be physically determined from the detector output current by either coherent signal detection or envelope detection methods, and the amplitude squared, A^2, can be determined by square law detection methods.

The Quadrature Model. The statistical models for detection of A and A^2 can be related to the heterodyne detector output current by first looking at the well known quadrature model (Ref 17:238). As can be seen from Fig. 10, one quadrature output is the real part of the complex current and the other is the imaginary part of the complex current. The statistics of the quadrature outputs can be

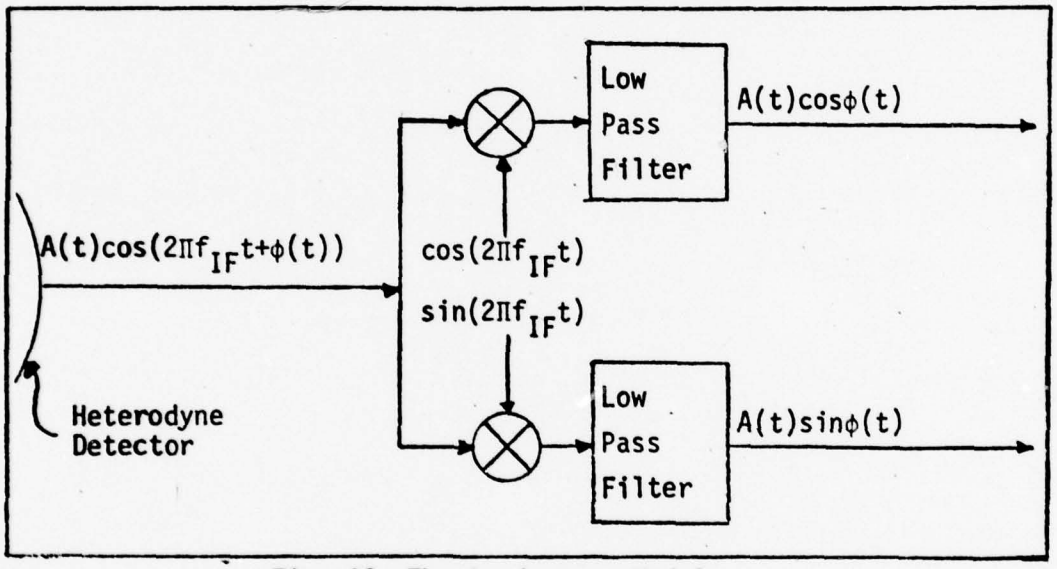


Fig. 10 The Quadrature Model

determined as follows. Beckman has shown, by using the classical random walk problem and the Central Limit Theorem that the real and imaginary parts of the scattered field are joint Gaussian random variables (Ref 5:124). From this result it is straightforwarded to show that the quadrature outputs are Gaussian random processes (Ref 10:504-509).

The results of Eq. (47) can be used to show that the covariance of I_r and I_i are equal as follows:

$$E[i(t)i(t')] = E[I_r(t)I_r(t')-I_i(t)I_i(t')+j\{I_r(t)I_i(t') + I_r(t')I_i(t)\}]=0 \quad (61)$$

which implies that for all t, t'

$$E[I_r(t)I_r(t')]=E[I_i(t)I_i(t')] \quad (62)$$

and

$$E[I_r(t)I_i(t')]=-E[I_r(t')I_i(t)] \quad (63)$$

The terms of Eqs. (62) and (63) can be related to the covariance of the complex current as follows:

$$E[i(t)i^*(t')] = E[I_r(t)I_r(t')+I_i(t)I_i(t')+j\{I_r(t)I_i(t')-I_r(t')I_i(t)\}]$$

$$= 2E[I_r(t)I_r(t')]+2jE[I_r(t)I_i(t')] \quad (64)$$

Since all the terms in the expression for the covariance of the complex current given by Eq. (54) are real, the cross correlation of I_r and I_i in Eq. (64) is zero and Eq. (64) becomes

$$E[i(t)i^*(t')]=2E[I_r(t)I_r(t')] \quad (65)$$

or

$$E[I_r(t)I_r(t') = \frac{1}{2}E[i(t)i^*(t')] \triangleq \frac{\sigma_i^2}{2} k_o(t,t') \quad (66)$$

where $k_o(t,t)=1$. From Eq. (63) it can be seen that I_r and I_i are identically distributed random processes. In particular, at $t=t'$ the variances of the quadratures are equal from Eq. (63), and they are equal to one half the variance of the complex current as shown by Eq. (66). The results of Eqs. (64) and (65) have shown that I_r and I_i are uncorrelated random processes, and because they are Gaussian, they are also statistically independent. Thus at this point it has been shown that the quadrature outputs are zero mean, statistically independent, identically distributed Gaussian random processes. Also, the distribution of these random processes has been related to the complex current by Eqs. (65) and (66).

Background Theory for Detection of A and A^2. The above model is now equivalent to the well known narrowband noise model (Ref 18:399-403). The amplitude squared of the current can be obtained from the quadrature model by squaring each quadrature output and adding together the results. The square root of this output is then the amplitude. This model is shown in Fig. 11. The first order, i.e. single sample, probability density of the amplitude is the Rayleigh probability density which is a well known transformation from the Gaussian probability density of the quadratures.

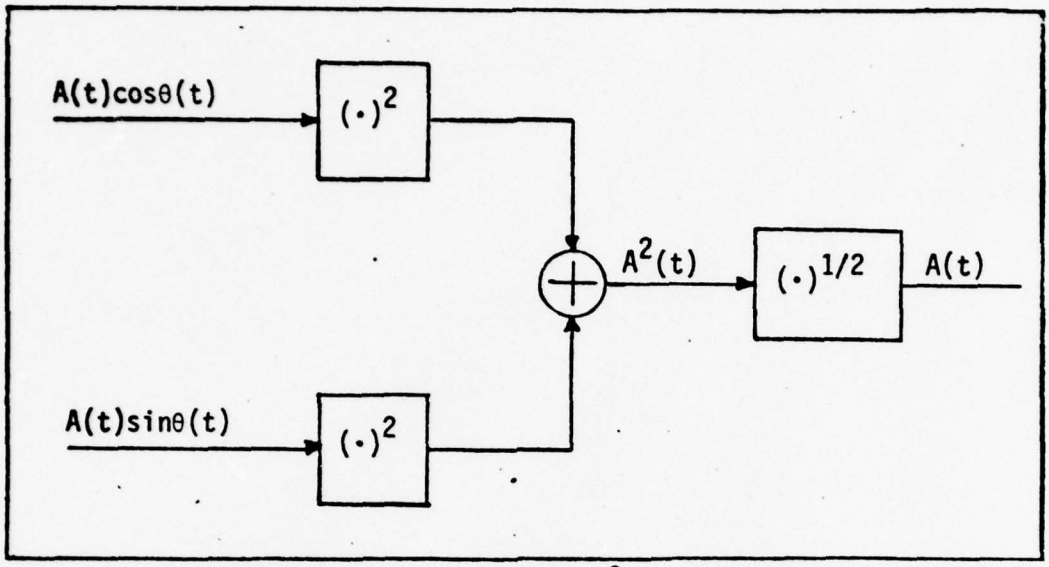


Fig. 11 Determination of A and A^2 from the Quadrature Outputs

The k^{th} moment of the amplitude from the Rayleigh density is defined as

$$E[A^k] = (2\sigma_r^2)^{k/2}\Gamma(\tfrac{k}{2} + 1)$$
$$= (\sigma_1^2)^{k/2}\ \Gamma(\tfrac{k}{2} + 1) \qquad (67)$$

where $\Gamma(\cdot)$ represent the Gamma function. These Rayleigh moments have been previously suggested for a heterodyne system but the details of the model were not presented (Ref 19:648-649).

A typical performance measure for a system is the signal to noise ratio, SNR. The SNR is defined as the ratio of the signal power to the noise power, or, in statistical terms, it is the square of the mean divided by the variance.

A SNR of less than one implies that the signal is dominated by the noise. A check of the SNRs for the two detection processes can easily be made using Eq. (67) as follows.

$$SNR_A = \frac{E^2[A(t)]}{\sigma^2_{A(t)}} = \frac{\frac{\Pi\sigma_r^2}{2}}{2\sigma_r^2 - \frac{\Pi\sigma_r^2}{2}} = \frac{\Pi}{4-\Pi} = 3.66 \qquad (68)$$

and

$$SNR_A2 = \frac{E^2[A(t)]}{\sigma^2_{A(t)}} = \frac{4\sigma_r^4}{8\sigma_r^4 - 4\sigma_r^4} = 1 \qquad (69)$$

As can be seen from the above two equations the SNRs are independent of all system parameters and thus are not a useful performance measure for system design purposes. In fact, the SNR represents a time independent measure of performance, whereas a more useful approach is to use the covariance function which includes the time dependence. The covariance of A is given as (Ref 18:403)

$$C_A(t,t') = \frac{\sigma_i^2}{2}\{2\underline{E}[k_o(t,t')] - [1-k_o^2(t,t')]\underline{K}[k_o(t,t')] - \frac{\Pi}{2}\} \qquad (70)$$

where $\underline{K}$ and $\underline{E}$ are the elliptical integrals of the first and second kind respectively. The covariance A^2 is much simpler and is (Ref 18:403)

$$C_A2(t,t') = \sigma_i^4 k_o^4(t,t') = [C_i(t,t')]^2 \qquad (71)$$

The information to develop the individual models for detection of A and A^2 is now available through the means from Eq. (67) and the covariance functions of Eqs. (70 and (71).

The Model for Detection of A^2. The model for A^2 will be discussed first because it is simpler and easier to interpret. From Eqs. (54) and (67) the mean of A^2 can be expressed in terms of the reflectance and system function as follows.

$$E[A^2(t)]=\sigma_i^2=B^2\int\int h(\alpha)h(\alpha')a(\alpha+vt)a(\alpha'+vt')P_\ell(\Delta\alpha)d\alpha d\alpha' \quad (72)$$

As previously noted, $P_\ell(\Delta\alpha)$ is very narrow with respect to changes in $h(\alpha)$ and $a(\alpha)$ so as an approximation it can be represented in terms of the Dirac delta function as follows.

$$P_\ell(\Delta\alpha) = C\delta(\Delta\alpha) \quad (73)$$

where $C = \int_{-\infty}^{\infty} P_\ell(\Delta\alpha)d\Delta\alpha$. The system function, $h(\alpha)$, is also symmetric so Eq. (69) becomes:

$$\begin{aligned} E[A^2(t)] &= CB^2 \int\int_{-\infty}^{\infty} h(-\alpha)h(-\alpha)a(\alpha+vt)a(\alpha'+vt')\delta(\alpha-\alpha')d\alpha d\alpha' \\ &= CB^2 \int_{-\infty}^{\infty} h^2(-\alpha)a^2(\alpha+vt)d\alpha \\ &= CB^2 \int_{-\infty}^{\infty} h^2(vt-x)a^2(x)dx \end{aligned} \quad (74)$$

Thus the mean of $A^2(t)$ can be represented by a linear system model of $a^2(x)$ convolved with $h^2(x)$. Again by using Eq. (54), the covariance of A^2 from Eq. (71) can be expressed in terms of the covariance of the complex current as follows:

$$C_A{}^2(t,t') = [B^2 \int\int_{-\infty}^{\infty} h(\alpha)h(\alpha')a(\alpha+vt)a(\alpha'+vt')P_\ell(\Delta\alpha+\Delta t)d\alpha d\alpha']^2$$

$$= [B^2 \int\int_{-\infty}^{\infty} h(vt-x)h(vt'-x')a(x)a(x')P_\ell(x-x')$$

$$dxdx']^2 \qquad (75)$$

the double integral in the above equation is identical to that obtained in computing the output correlation of a filter with an impulse response h(x) driven by zero mean noise of correlation $R_n(x,x')=a(x)a(x')P_\ell(x-x')$. The square of the double integral in Eq. (75) simply means that the noise can be represented by the product of two noise processes that are identically distributed and statistically independent. In contrast to many other noise models the above model is signal (i.e. a(x)) dependent. The second moment model for square law detection is shown in Fig. 12.

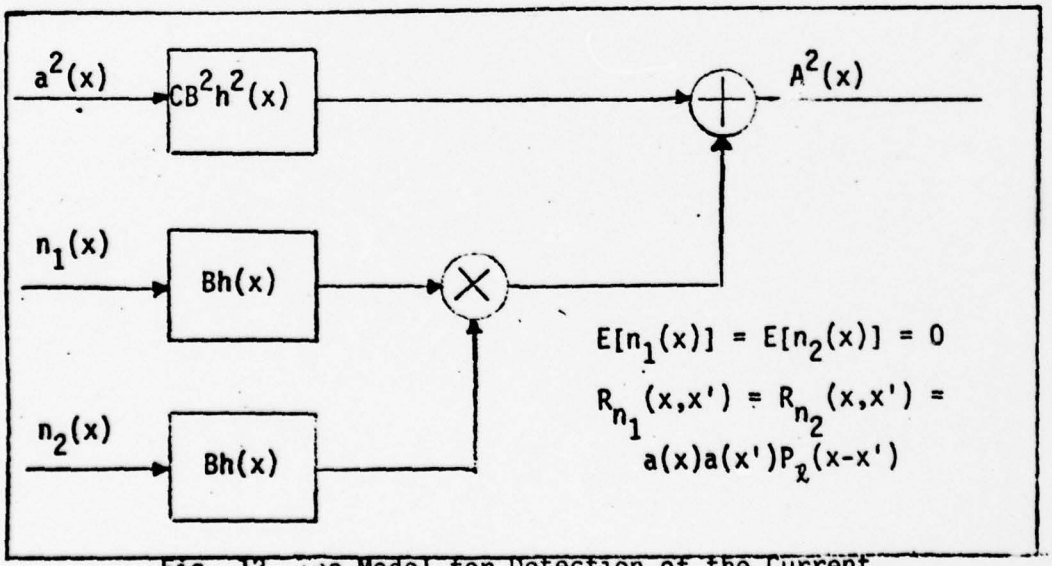


Fig. 12 The Model for Detection of the Current Amplitude Squared

The speckle noise model presented above can be easily modified to include the quantum noise effects that were neglected in the detector output current given by Eq. (21). It has been shown that the output noise statistics for a heterodyne detector can be represented as a Gaussian random process (Ref 12:189). Thus these statistics are compatible with the model presented here and the detector noise terms can be included simply by adding the appropriate terms to the speckle noise representation in Eq. (75).

Several things can be noted from the model for A^2. The output, A^2, can be considered either a spatial signal in the variable x or a temporal signal in the variable t, where the relationship between the two variables is x=vt. The temporal Fourier transform of $A^2(t)$ using Eq. (74) is

$$F_t[E[A^2(t)]] = \frac{B^2 c}{|v|} H'(\frac{f}{v})A'(\frac{f}{v}) \qquad (76)$$

where $H'(f)=F[h^2(t)]$ and $A'(f)=F[a^2(t)]$. From Eq. (76) is can be seen that the frequency content of the output spectrum will broaden as v increases. Thus the bandwidth of the electronics that process the output must be scaled by v to maintain the desired frequency content a^2 in the final image.

The model for $E[A^2(x)]$ is also identical to the result discussed by Goodman for an incoherent imaging system (Ref 7:109). (In two dimensions the Fourier transform of $h^2(x,y)$ divided by the same transform evaluated at frequencies $f_x=f_y=0$ is commonly called the optical transfer function, OTF.)

Thus, square law detection can be thought of as an incoherent imaging system with an additive noise term given by Eq. (75).

The spatial filtering by $h^2(x)$ and thus the system function, $h(x)$, can be seen by taking the spatial Fourier transform of $E[A^2(x)]$ from Eq. (71) as follows:

$$F_x[E[A^2(x)]] = B^2CA'(f_x)H'(f_x)$$
$$= B^2C[A'(f_x)][H(f_x)*H(f_x)] \qquad (77)$$

where $H(f_x)=F_x[h(x)]$. Since the Fourier transform has an inverse effect on the width of a function, the wider the system function in space the narrower $H(f_x)$ becomes. As $H(f_x)$ becomes narrower so does the convolution of $H(f_x)$ with itself and thus more of the high frequency content of $a^2(x)$ is filtered out. Another way to see this filtering effect is to look at the resolution of two point sources of reflectivity that are separated by a distance d, i.e. $a^2(x)=\delta(x)+\delta(x-d)$. Then from Eq. (74):

$$E[A^2(t)] = B^2C \int_{-\infty}^{\infty} h^2(vt-x)[\delta(x)+\delta(x-d)]dx$$
$$= B^2Ch^2(vt)+B^2Ch^2(vt+d) \qquad (78)$$

As an example, it can be assumed that $h^2(x)$ is a Gaussian amplitude function (consistent with a Gaussian laser beam), and then the resolution limit can be picked as the point where the peak of one function is at the e^{-1} point of the other. Then from Eq. (78) it can easily be seen that d must be the distance at which $h^2(x)$ is at it's e^{-1} point if the two points are to be resolved. So again the wider system

function in space the worse the resolution ability of the system. This is a very intuitive result since the detector measures an average of the reflectance points each weighted by the value of the system function at that point. The wider h(x) is then the more even this weighting becomes over the width of h(x). Thus, if two points of equal reflectivity are to be resolved by the system, they must be separated by a distance large enough such that the difference in the weighting of each point is large enough to cause a distinguishable effect in the detector output.

The effect of h(x) on the mean does not tell the complete story since h(x) also effects the covariance of A^2, ie.e the fluctuations of $A^2(x)$. The covariance of A^2 from Eq. (75) is nonstationary, but an indication of the correlation distance can be determined from the correlation distance of the complex current given by Eqs. (55) and (56). The result of squaring the complex current correlation function is to reduce the maximum correlation distance of Eq. (56) slightly. Still, it can be seen that the wider the system function the longer the maximum correlation distance.

The square root of the covariance at t=t from Eq. (75), i.e. the square root of the variance, represents the rms variation from the mean due to the "noise". This variation can the thought of as the contrast variations in the output image that are due to the rough surface (speckle) noise. Also, the correlation distance represents the average period

over which this noise process is related or does not change "very much". Thus, the the correlation distance can be thought of as the average speckle cell size in the resulting image, and it is directly related to the width of the system function, h(x), as was shown by Eq. (56).

The effect of the system function on the noise can also be seen by looking at the noise power spectral density. The Fourier transform of the output covariance with respect to $v\Delta t$ is called the power spectral density, $S(f_x)$ (Ref 20: 347). It represents the noise power per spatial frequency that passes through the system. The total output noise power is found by integrating $S(f_x)$ over all frequencies. The power in a particular frequency band is found by simply integrating $S(f_x)$ over that band of frequencies.

The covariance of A^2 given by Eq. (75) is nonstationary so strictly speaking it is not subject to Fourier analysis. But if the reflectance is considered nearly constant (or slowly varying) then the power spectral density of A^2 is

$$S_{A^2}(f_x) = B^2a^2P_{\ell F}(f_x)|H(f_x)|^2 * B^2a^2P_{\ell F}(f_x)|H(f_x)|^2 \qquad (79)$$

where $P_{\ell F}(f_x)=F[P_\ell(\Delta x)]$. Because $P_\ell(\Delta x)$ is very narrow compared to h(x), the spatial frequency spectrum of $P_{\ell F}(f_x)$ will be wideband or "white" compared to $H(f_x)$. Or, by again approximating $P_\ell(\Delta x)$ as $C\delta(\Delta x)$ as in Eq. (73), Eq. (79) can be written as:

$$S_{A^2}(f_x) = CB^4a^4[|H(f_x)|^2_*|H(f_x)|^2] \qquad (80)$$

Thus, as h(x) becomes wider, $|H(f_x)|^2$ becomes narrower, and the total noise power out will decrease because of the smaller non-zero ranges over which $S_{A^2}(f_x)$ will exist.

This completes the analysis of the A^2 model. It has been shown by several approaches that the resolution of the reflectance information is reduced as the system function is widened to reduce the noise power or noise flucuations. The model for envelope detection will now be developed to see how the system function affects that method of detection.

The Model for Detection of A. The model for the measurement of the amplitude is much more difficult because of the expression for the covariance and the square root involved. The mean of the amplitude from Eqs. (54) and 967) is:

$$E[A(t)] = B\frac{\Pi}{2}[\int\int h(\alpha)h(\alpha')a(\alpha+vt)a(\alpha'+vt)P_\ell(\Delta\alpha)d\alpha d\alpha']^{1/2}$$

$$= \frac{B\ \Pi}{2}C^{1/2}[\int h^2(\alpha)a^2(\alpha+vt)dx]^{1/2}$$

$$= \frac{B\ \Pi}{2}C^{1/2}[\int h^2(vt-x)a^2(x)dx]^{1/2} \qquad (81)$$

This is the same expression (within a constant) as the square root of the mean of A^2 from Eq. (74). Therefore the comments following Eqs. (76) and (77) regarding the electronics bandwidth and the system function apply for the detection of the amplitude, too.

The covariance of A from Eq. (70) was expressed in terms of the elliptical integrals of $\underline{K}$ and $\underline{E}$ as follows:

$$C_A(t,t') = \frac{\sigma_i^2}{2} \{2\underline{E}[k_o(t,t')] - [1-k_o^2(t,t')]\underline{K}[k_o(t,t')] - \frac{\pi}{2}\} \quad (70)$$

The elliptical integrals can be represented by the following series (Ref 21:310)

$$\underline{K}(x) = \frac{\pi}{2} \{1 + \sum_{i=1}^{\infty} [\frac{1\cdot3\cdot5\cdots(2i-1)}{2\cdot4\cdot6\cdots(2j)}]^2 x^{2i}\} \quad (82)$$

and

$$\underline{E}(x) = \frac{\pi}{2} \{1 - \sum_{j=1}^{\infty} [\frac{1\cdot3\cdot5\cdots(2j-1)}{2\cdot4\cdot6\cdots(2j)}]^2 \frac{x^{2j}}{(2j-1)}\} \quad (83)$$

The terms in the outer brackets of Eq. (70) can be combined using $x=k_o(t,t')$ as follows:

$$\pi\{1 - \sum_{j=1}^{\infty} [\frac{1\cdot3\cdot5\cdots\cdot(2j-1)}{2\cdot4\cdot6\cdots\cdot(2j)}]^2 \frac{x2j}{(2j-1)} - (1-x^2)(\frac{\pi}{2})\{1 + \sum_{j=1}^{\infty}$$

$$[\frac{1\cdot3\cdot5\cdots\cdot(2j-1)}{2\cdot4\cdot6\cdots\cdot(2j)}]^2 x^{2j}\} - \frac{\pi}{2}$$

$$= \pi \sum_{j-1}^{\infty} [\frac{1\cdot3\cdot5\cdots\cdot(2j-1}{2\cdot4\cdot6\cdots\cdot(2j)}]^2 [(\frac{2j}{2j-1})^2(\frac{1}{2}) - \frac{2j+1}{4j-2}] x^{2j} \quad (84)$$

Eq. (84) can now be evaluated explicitly for the first terms in the series as follows

$$\frac{\pi}{8} x^2 + \frac{\pi}{8}(\frac{1}{16}) x^4 + \frac{\pi}{8}(\frac{1}{64}) x^6 + \frac{\pi}{8}(\frac{25}{4096}) x^8 + \cdots\cdots \quad (85)$$

so the covariance of the amplitude becomes:

$$C_A(t,t') = \frac{\sigma_i^2\pi}{16}[k_o^2(t,t')+\frac{1}{16}k_o^4(t,t')+\frac{1}{64}k_o^6(t,t')+\frac{25}{4096}k_o^8(t,t') + \cdots]=\frac{\sigma_i^2\pi}{16}[(\frac{C_i(t,t')}{\sigma_i^2})^2+\frac{1}{16}(\frac{C_i(t,t')}{\sigma_i^2})^4 + \frac{1}{64} (\frac{C_i(t,t')}{\sigma_i^2})^6+\frac{25}{4096} (\frac{C_i(t,t')}{\sigma_i^2})^8+\cdots] \quad (86)$$

The first term, except for the constants, is the same as the covariance of A^2 from Eq. (71), where the square of $C_i(t,t')$ implied that the noise could be modeled as the product of two independent noise processes. In Eq. (86) the sum of the higher order powers of $C_i(t,t')$ implies that the noise can be molded as a sum of independent noise processes. Additionally each term in the sum is itself a product of m independent noise processes where m is equal to the power of the $C_i(t,t')$ term involved.

For any t' not equal to t in Eq. (86) the term $C_i(t,t')$ is less than σ_i^2 so the terms of Eq. (86) are rapidly decreasing with the higher powers of $\frac{C_i(t,t')}{\sigma_i^2}$. As the coherence length of $C_i(t,t')$ of Eq. (56) is approached $\frac{C_i(t,t')}{\sigma_i^2}$ becomes very small and Eq. (86) can be quite accurately approximated by the first term. Except for the constants this approximation yields the same form as the covariance of A^2 from Eq. (75). Thus the coherence distance can be considered to be approximately the same for both methods of detection.

If the power spectral density of Eq. (86) is determined in a manner similar to the case for A^2 from Eq. (80), the result would be a series of double, quadruple, and higher order convolutions. This means that the noise power is unlimited in frequency, although it is reduced in amplitude at each higher order convolution. In fact, if the value of the first term of Eq. (86) at t=t' is compared to the variance of A using Eq. (67), the result is:

$$\frac{(\frac{\sigma_{i\Pi}^2}{16})}{\frac{\sigma_i^2}{2}(2-\frac{\Pi}{2})} = \frac{\Pi}{8}\left(\frac{2}{4-\Pi}\right) = .915 \qquad (87)$$

Eq. (87) shows that 91.5% of the noise power is concentrated in the first term of the covariance of A when the covariance function is at it's maximum value, i.e. at t=t'. It was also determined in the previous paragraph that the first term was an excellent approximation for the covariance of A when the covariance is small, i.e. at the coherence time. Thus, as a first approximation the noise covariance function can be represented as:

$$C_A(t,t') = \frac{\Pi[C_i(t,t')]^2}{16\ \sigma_i^2} \qquad (88)$$

for all t,t'. This approximation is in addition to the more accurate first term approximation that was given for the coherence length. Again, except for the constants, the noise representation is now the same as that for A^2 given by Eq.

(71). With this approximation the model for detection of A is given in Fig. 13.

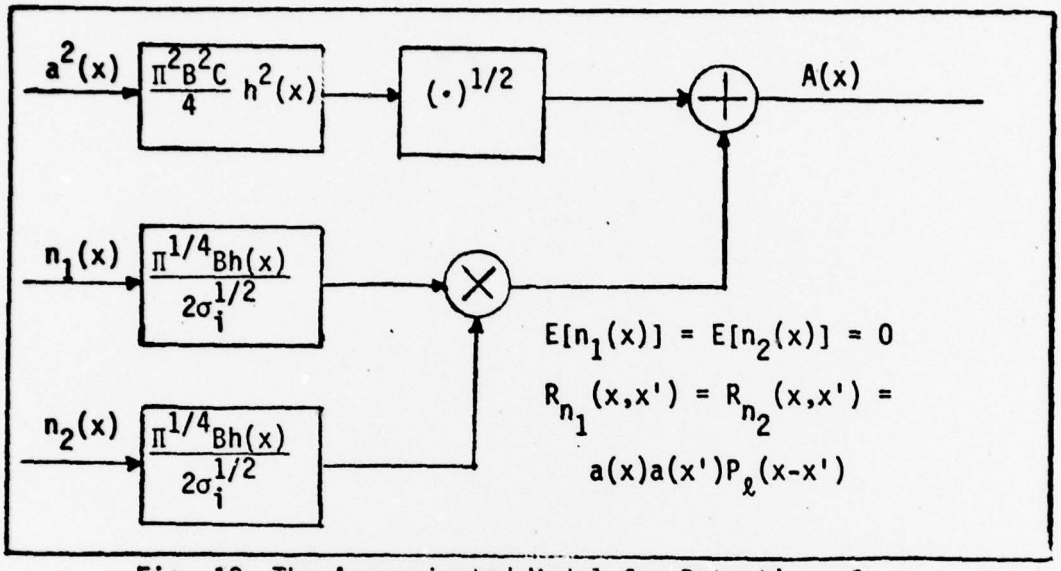


Fig. 13 The Approximated Model for Detection of the Current Amplitude

The system parameters now have the same effect on the resulting image in both the A and A^2 models although the final image is not the same because of the square root of the mean in the model for detection of A. In fact, the mean of A^2 is proportional to a^2, i.e., the square of the field reflectivity, and thus is directly related to the intensity of the reflected field. Since the human eye also measures intensity, the A^2 image is proportional to the reflectivity term that people are familiar with. On the other hand, the mean of A is proportional to the field reflectivity, a, and the result is an image that may not be natural to the human observer. However, this image is still a valid representation of the surface characteristics.

IV. SUMMARY

Conclusions

As was stated in the background section, there is a great deal of information available in the literature concerning speckle as it relates to imaging systems that make intensity measurements. Very little information was available on modeling the output of an optical heterodyne line-scan imaging system. The purpose of this thesis was to develop such a model that included the effects of the speckle noise, which is caused by reflection of the field from a rough surface object. This rough surface, however, is necessary in the scanning system to provide backscattered radiation to the detector, otherwise the detector would only receive a return signal the few times the laser beam was normally incident to the object surface. The methods of detecting either the amplitude or amplitude squared of the current from the heterodyne detector have been modeled in this thesis. The amplitude of the current is easily measured in an actual system by envelope detection or it can be detected by more sophisticated coherent detection methods. The amplitude squared of the current can be determined by use of common square law detectors.

Because the detector output is the average of all of the reflectance points within the laser beam, it was argued that the significant changes in the detector output occurred as a function of the scanning direction of the system. The

reflectance at each point in the scanning direction could be considered equal to the average of the reflectance across the width of the beam perpendicular to the scanning direction at that point. Thus, the system model was developed in the scanning direction only. The one dimensional Huygens-Fresnel integral was used to propagate the laser output to the object's surface and the reflected field back to the detector. The laser and detector were modeled as being stationary in a fixed coordinate system while the surface characteristics were moved beneath the laser beam. It was pointed out that the effects of beam spreading and changing surface velocity, that were ignored in this model but which occur in the actual system, could be determined from this model simply by varying the appropriate parameters. In the development of the system model, the object's surface was considered to be a zero mean Gaussian random process, but it was later argued that the results were typical of any naturally rough surface. It was shown that the rms roughness of the surface could be compared directly to the optical wavelength and that many surfaces are rough compared to optical wavelengths. A system function was defined which represented the combined effect of the detector field of view and the laser beam amplitude function. Then the complex current was used in determining the statistics of the optical detector's output and it was shown that the mean signal was zero when the objects surface was rough compared

to an optical wavelength. It was also shown that the correlation function of the reflected field was very narrow, on the order of tenths and hundredths of a millimeter. This narrow correlation function meant that the reflected field was now spatially coherent over just a very short distance. This fact allowed the quadratic phase terms to be neglected which resulted in a model that was the same for both far field and near field cases.

Because the mean of the detector output current was zero, a mehtod of detection the amplitude or amplitude squared of the current was included. The amplitude is related to the sum of the squares of the real and imaginary parts of the current so the quadrature model was presented. The quadrature outputs were shown to be identically distributed, zero mean joint Gaussian random processes. Based on this result, it was concluded that the first order density of the amplitude was Rayleigh and that the model was now similar to the well known narrowband noise model. The signal to noise ratio for each detection method was calculated from the moments of the Rayleigh density but in both cases it was independent of the system parameters.

However, a second moment model for each detection process, which included the system parameters, was developed. The respective mean (signal) and covariance (noise) functions were all expressed in terms of the previously determined covariance function of the complex current. The amplitude

squared signal model was shown to be identical to the linear system model for an incoherent imaging system where the Fourier Transform of the system function squared represents the well known Optical Transfer Function. It was shown that the resolution ability of the system degraded as the width of system function was increased in space. This was intuitively pleasing since an increase in the width of the system function causes more reflectance points to be included in the averaging process and thus the effect of each individual reflectance point becomes smaller. The amplitude signal model was developed and shown to be identical to the amplitude squared signal model except for some constants and the final square root of the output. The filtering effects of the system function were the same for both models.

In each model, the noise covariance was shown to be represented by the square of the complex current correlation function and unlike some common noise processes it was a function of the reflectivity signal. The models provided considerable information about the speckle noise. The coherence length of the noise process represents the period that noise is related and thus corresponds to the average speckle cell size in the image. This correlation distance was determined to be equal to the width of the system function except that when the reflectivity varied significantly over the same distance, it could become smaller. The contrast in the image due to the speckle noise was given by the square root of the variance and could be determined from

the noise representation in the models. The models show how the system parameters affect the signal and the speckle noise and they provide the basis for developing signal processing methods that will optimize the desired image. Also, it was shown that the common heterodyne detector noise models could be easily added to the speckle noise models presented here.

Recommendations

Although the models developed in this thesis describe the speckle effects, they do not provide a definite solution to the problem of producing the "best" image in the presence of speckle noise. It is recommended that optimization techniques be applied to the models to determine what signal processing could be done to provide satisfactory system performance. It would be helpful to know what the expected spatial frequency content of the reflectance is so that the reflectance signal power spectrum could be compared to the noise power spectral density. Then a minimum acceptable resolution criterion could be developed, and an appropriate filter determined that would yield the desired resolution while filtering those frequencies that reduce the image quality. Also, this would allow comparisons to be made between the two signal detection models to determine which detection method would yield the best performance. Of course comparison of the models developed here with additional experimental data would serve to validate them. Finally,

the development of a similar model for optical direct detection line-scan imaging systems would provide the basis needed for determining which type of system should be further developed.

Bibliography

1. Oliver, B. M. "Sparkling Spots and Random Diffraction." Proceedings IEEE, 51: 220-221 (January-March 1963).

2. Rigden, J. D. and E. I. Gordon. "The Granularity of Scattered Optical Maser Light." Proceeding I.R.E., 50: 2367-2368 (October-December 1962).

3. Journal of the Optical Society of America, 66: (November 1976).

4. Dainty, J. C., et al. Topics in Applied Physics, 9, New York: Springer-Verlag, 1975.

5. Beckmann, P. and Spizzichino, A. The Scattering of Electromagnetic Waves from Rough Surfaces. New York: The Macmillan Company, 1963.

6. Goodman, J. W. "Some Effects of Target-Induced Scintillation on Optical Radar Performance." Proceeding of the IEEE, 53: 1688-1700 (November 1965).

7. Goodman, Joseph. Introduction to Fourier Optics. St. Louis: McGraw-Hill Book Company, 1968.

8. Seigman, A. E. An Introduction to Lasers and Masers. St. Louis: McGraw-Hill Book Company, 1971.

9. Hecht, E. and Zajac, A. Optics. Reading, Mass.: Addison-Wesley Publishing Company, 1975.

10. Davenport, W. B. Jr. Probability and Random Processes. St. Louis: McGraw-Hill Book Company, 1970.

11. Corcoran, V. "Directional Characteristics in Optical Heterodyne Detection Processes." Journal of Applied Physics, 36: 1819-1825 (June 1965).

12. Pratt, William K. Laser Communication Systems. New York: John Wiley and Sons, Inc., 1969.

13. Jacobs, S. F. and Rabinowitz, P. J. "Optical Heterodyning with a CW Gaseous Laser" in Quantum Electronics Proceeding of the Third International Congress (1963), edited by P. Grivet and N. Bloembergen. New York: Columbia University Press, 1964.

14. Miller, M. G., et al. "Second-order Statistics of Laser-speckle Patterns." Journal of the Optical Society of America, 65: 779-785 (July 1975).

15. Handbook of tables for Applied Engineering Science, by R. Bolz and G. Tuve. Cleveland, Ohio: The Chemical Rubber Company Press, 1976.

16. Kurtz, C. N. "Transmittance Characteristics of Surface Diffusers and Design of Nearly Band-Limited Binary Diffusers." Journal of the Optical Society of America, 62: 982-989 (August 1972).

17. Ziemer, R. E. and W. H. Tranter. Principles of Communications. Boston: Houghton Mifflin Compnay, 1976.

18. Middleton, D. An Introduction to Statistical Communication Theory. New York: McGraw-Hill Book Company, 1960.

19. Gould G., et al. "Coherent Detection of Light Scattered from a Diffusely Reflecting Surface." Applied Optics, 3: 648-649 (May 1964).

20. Papoulis, A. Probability, Random Variables, and Stochastic Processes. St. Louis: McGraw-Hill Book Company, 1965.

21. Bendat, Julis. Principles and Applications of Random Noise Theory. New York: John Wiley and Sons, Inc., 1958.

22. Papoulis, Athanasios. Systems and Transforms with Applications in Optics. St. Louis: McGraw-Hill Book Company, 1968.

VITA

Barry W. Lyons was born on 14 October 1946 in Galesburg, Illinois to Bernard W. and Francis R. Lyons. He graduated from Alexis High School in 1964 and attended Western Illinois University from 1964 to 1966. In February 1966 he enlisted in the United States Air Force and in November 1966 he graduated from the Automatic Flight Control Systems School at Chanute AFB, Illinois. On 5 February 1967 he was married to Sharon S. Lee. During the next four years he served tours at Luke AFB, Arizona; Bien Hoa AFB, Vietnam; Cannon AFB, New Mexico; and again at Chanute AFB, Illinois. In February 1971 he was accepted into the Airman Education and Commissioning Program and attended the University of Illinois where he graduated in 1973 with a Bachelor of Science degree in Electrical Engineering. On 10 May 1973 he was commissioned a 2nd Lieutenant through OTS and assigned to the National Security Agency, Ft. Meade, Maryland. In June 1976 he entered the Masters of Science Electro-Optics program in the School of Engineering at the Air Force Institute of Technology.

Permanent Address: Rural Route 1
Rio, Illinois 61472

UNCLASSIFIED

SECURITY CLASSIFICATION OF THIS PAGE *(When Data Entered)*

REPORT DOCUMENTATION PAGE		READ INSTRUCTIONS BEFORE COMPLETING FORM
1. REPORT NUMBER AFIT/GEO/EE/77-4	2. GOVT ACCESSION NO.	3. RECIPIENT'S CATALOG NUMBER
4. TITLE *(and Subtitle)* A SPECKLE NOISE MODEL FOR OPTICAL HETERODYNE LINE-SCAN IMAGERY		5. TYPE OF REPORT & PERIOD COVERED MS Thesis 6. PERFORMING ORG. REPORT NUMBER
7. AUTHOR(s) Barry W. Lyons Captain, USAF		8. CONTRACT OR GRANT NUMBER(s)
9. PERFORMING ORGANIZATION NAME AND ADDRESS Air Force Institute of Technology (AFIT-EN Wright-Patterson AFB, Ohio 45433		10. PROGRAM ELEMENT, PROJECT, TASK AREA & WORK UNIT NUMBERS
11. CONTROLLING OFFICE NAME AND ADDRESS Electro-Optics and Reconnaissance Branch (AFAL/RWI) Air Force Avionics Laboratory Wright-Patterson AFB, Ohio 45433		12. REPORT DATE December, 1977 13. NUMBER OF PAGES 71
14. MONITORING AGENCY NAME & ADDRESS*(if different from Controlling Office)*		15. SECURITY CLASS. *(of this report)* Unclassified 15a. DECLASSIFICATION/DOWNGRADING SCHEDULE

16. DISTRIBUTION STATEMENT *(of this Report)*

Approved for public release; distribution unlimited.

17. DISTRIBUTION STATEMENT *(of the abstract entered in Block 20, if different from Report)*

18. SUPPLEMENTARY NOTES

Approved for public release IAW AFR 190-17
JERRAL F. GUESS, Captain, USAF
Director of Information

19. KEY WORDS *(Continue on reverse side if necessary and identify by block number)*

Line scanning
Terrain mapping
Lasers
Heterodyning
Images
Reflectivity
Scattering

20. ABSTRACT *(Continue on reverse side if necessary and identify by block number)*

An imaging system that consists of a laser scanning a surface and a heterodyne receiver that measures the backscattered field is considered. When the scanned surface is rough compared to the wavelength of the incident laser beam the coherent properties of the laser beam are destroyed in the backscattered field. The result is a noise in the image that is referred to as "speckle".

The rough surface is modeled by multiplying the incident scalar field by a reflectance term and a random phase term. The random phase is modeled as a

DD FORM 1 JAN 73 1473 EDITION OF 1 NOV 65 IS OBSOLETE

UNCLASSIFIED

SECURITY CLASSIFICATION OF THIS PAGE *(When Data Entered)*

012 225

random process whose mean, variance, and correlation distance are functions of the rough surface. The statistics of the amplitude and amplitude squared of the current from the optical detector are developed in a manner similar to the well known narrowband noise model. Second moment models for detection of the amplitude or amplitude squared are presented. The mean and covariance functions of each model are related to the field correlation function, the reflectance of the surface, and the system parameters. The noise models describe both the average speckle cell size in the image and the contrast in the image caused by the speckle noise.